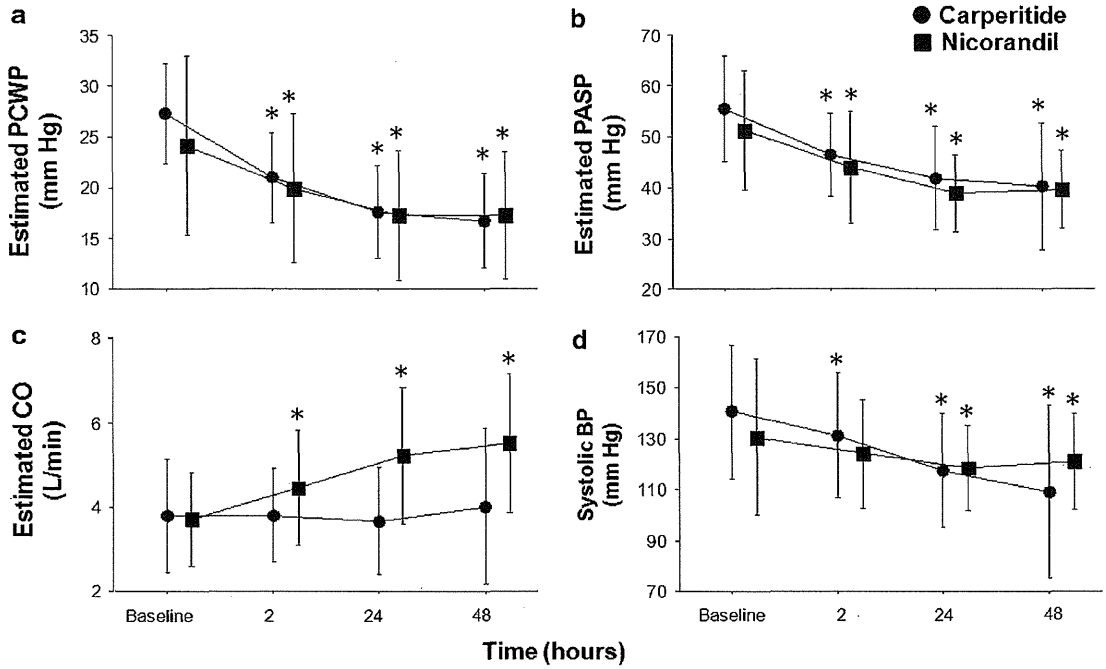

Fig. 1 Changes in estimated PCWP (**a**), estimated PASP (**b**), estimated CO (**c**), and systolic BP (**d**) during 48-h carperitide or nicorandil infusion. *$P < 0.05$ versus baseline by Dunnett's multiple comparison method. *BP* blood pressure, *CO* cardiac output, *PASP* pulmonary artery systolic pressure, *PCWP* pulmonary capillary wedge pressure

nicorandil infusion (130.9 ± 30.5 to 121.5 ± 18.7 mmHg, $P < 0.05$; Fig. 1d). The average dose of intravenous nicorandil was 0.161 ± 0.054 mg/kg/h.

Differences in hemodynamic responses between carperitide and nicorandil

Percent changes in hemodynamic parameters from baseline after 48 h of carperitide or nicorandil infusion are shown in Fig. 2. Systolic BP decreased significantly more in the carperitide group than in the nicorandil group (22.1 ± 20.0 % vs 5.3 ± 10.4 %, $P = 0.003$). The improvement in estimated PCWP was superior in the carperitide group to that of the nicorandil group (38.2 ± 14.5 % vs 26.5 ± 18.3 %, $P = 0.036$), while the improvement in estimated CO was greater in the nicorandil group than in the carperitide group (52.1 ± 33.5 % vs 11.4 ± 36.9 %, $P = 0.001$). There were no significant differences between the two groups with respect to changes in diastolic BP, heart rate, and estimated PASP. Urine output from baseline to 24 h of study-drug infusion was significantly greater in the carperitide group than in the nicorandil group (2353 ± 939 vs 1708 ± 566 ml, $P = 0.015$). Urine output for 48 h of study-drug infusion was also greater in the carperitide group than in the

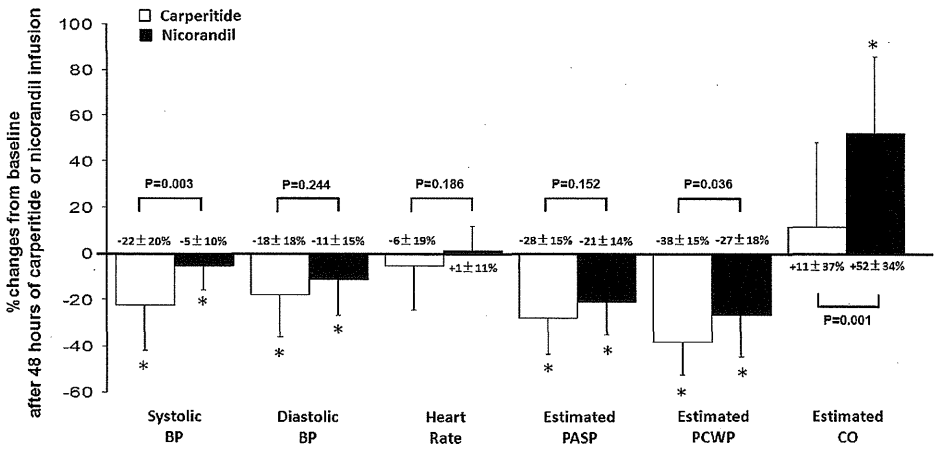

Fig. 2 Percent changes in systolic BP, diastolic BP, heart rate, estimated PASP, estimated PCWP, and estimated CO after 48-h carperitide or nicorandil infusion (versus baseline). *$P < 0.05$ versus baseline by Dunnett's multiple comparison method. *BP* blood pressure, *CO* cardiac output, *PASP* pulmonary artery systolic pressure, *PCWP* pulmonary capillary wedge pressure

nicorandil group (4203 ± 1542 vs 3627 ± 1074 ml), and the total dose of intravenous furosemide for 48 h tended to be smaller in the carperitide group than in the nicorandil group (29.0 ± 35.9 vs 40.2 ± 31.1 mg), but this was not statistically significant ($P = 0.189$ and $P = 0.313$, respectively). A trend for a more favorable change in creatinine level was observed in the carperitide group compared with the nicorandil group (+9.8 ± 27.3 % vs +16.8 ± 76.0 %), and the improvement in B-type natriuretic peptide levels was greater in the nicorandil group than in the carperitide group (−53.3 ± 32.2 % vs −45.3 ± 30.8 %); however, these differences were not statistically significant ($P = 0.709$ and $P = 0.439$, respectively).

Adverse events

Hypotension (systolic BP <90 mmHg) during 48 h of carperitide infusion was observed in three patients, which was successfully managed with dose reduction of this drug. There were two episodes of headache during the 48-h nicorandil infusion, which were successfully managed with a nonsteroidal anti-inflammatory drug. There were no episodes of recurrent dyspnea or arrhythmia in both groups. Infusion was therefore continued for 48 h in all study patients.

Discussion

In this study, we assessed the difference in hemodynamic response between carperitide and nicorandil in patients with AHFS. While both carperitide and nicorandil significantly improved hemodynamic parameters, the improvement in estimated PCWP was greater in the carperitide group and the improvement in estimated CO was superior in the nicorandil group. The carperitide group had a trend toward a higher urine output and lower total dose of intravenous furosemide over 48 h compared with the nicorandil group.

Nicorandil has a double cellular mechanism of action, acting both as an adenosine triphosphate-sensitive potassium channel activator and exhibiting a nitrate-like effect, which may explain its combined arterial and venous vasodilatory effects [9, 10, 21–23]. Dilation of the arterial resistance vessels reduces afterload and allows the left ventricle to eject more blood. The nitrate-like effect is primarily believed to affect the venous system and increase venous capacitance, and reduces congestion. This double effect might explain the hemodynamic effects observed in this study, i.e., a reduction in estimated PCWP and increase in estimated CO.

Carperitide is a cyclic peptide consisting of 28 amino acid residues and is called α-human atrial natriuretic peptide, which was isolated from the human atrium, and identified and synthesized by genetic recombination [24]. Carperitide has been clinically used for the management of AHFS, because of its pharmacological actions of vasodilation that reduce both preload and afterload, as well as having a natriuretic action [5, 25]. In addition, carperitide inhibits the renin–angiotensin–aldosterone and sympathetic nervous systems, which are believed to be related to the development, sustenance, and progression of heart failure [26, 27]. Therefore, carperitide may have a mechanism of action related to the pathology of AHFS. The reduction in systolic BP and PCWP observed in this study might have resulted from the vasodilator effect of carperitide. Furthermore, volume (preload) reduction by the natriuretic action of carperitide could have contributed to hemodynamic differences between carperitide and nicorandil observed in this study, i.e., the greater reduction in systolic BP and PCWP and no improvement of CO in the carperitide group. In fact, urine output over 24 h was significantly greater in the carperitide group than in the nicorandil group, although the total dose of intravenous furosemide tended to be smaller in the carperitide group. Further studies are required to investigate the exact mechanism responsible for the differences in hemodynamic responses between carperitide and nicorandil observed in this study.

Early management of AHFS is critical, but the current guidelines do not address the early clinical assessment and treatment of this syndrome. Recently, two or three categories of early-phase AHFS have been suggested by numerous researchers, mainly according to the patient's BP at the time of presentation [28, 29]. One type of AHFS is characterized by an elevation in systolic BP. High BP rapidly develops, and is related to high filling pressures and increased sympathetic tone; this results in the redistribution of systemic fluids and the activation of neurohormonal factors. Symptoms in these patients usually develop abruptly, and patients suffer pulmonary rather than systemic congestion. This type of heart failure is referred to as "vascular" failure or "hypertensive" AHFS [28, 29]. The other type of heart failure is characterized by normal or low BP. These patients show symptoms that gradually develop over several days, and have significant systemic congestion. This type of heart failure is referred to as "cardiac" failure or "normotensive–hypotensive" AHFS [28, 29]. Since vasodilators are not recommended as first-line therapy in hypotensive AHFS, vasodilation therapy is recommended in hypertensive and normotensive AHFS. In the current study, systolic BP and filling pressures (i.e., PCWP) had a greater decrease in the carperitide group than in the nicorandil group. In addition, a previous study revealed that a cutoff value of >120 mmHg for systolic BP had a sensitivity of 94 % and a specificity of 86 % for predicting

a good response to initial carperitide therapy [30]. Furthermore, the neurohormonal effect of carperitide, such as inhibition of the sympathetic nervous system, could attenuate the activation of neurohormonal factors in hypertensive AHFS. Using carperitide as first-line treatment in hypertensive AHFS could thus lead to favorable results. By contrast, the improvement in CO was greater and the change in systolic BP was smaller in the nicorandil group than in the carperitide group in the present study. Therefore, using nicorandil as a first-line treatment in normotensive AHFS could lead to favorable results. On the other hand, carperitide showed a tendency to have better diuretic activity, and the choice of carperitide could be useful for the treatment of normotensive AHFS with excessive volume overload under close monitoring to avoid hypotension. Furthermore, a recent case report describes the efficiency of a combination of low-dose carperitide and nicorandil in patients with AHFS and borderline BP (i.e., low to normal) [31]. The choice of vasodilators in normotensive AHFS patients, who are often difficult to manage, is controversial. This remains an important area of future research.

Limitations

The results of the present study have several limitations in the methodology. First, this was a single-center study with a small sample size. In addition, our study population was specifically selected to represent patients in whom echocardiography could be accurately performed in the urgent phase of AHFS. Second, we used transthoracic Doppler echocardiography to assess hemodynamic parameters in the study population. Pulmonary artery catheterization yields valuable hemodynamic findings, including filling pressures and CO, in patients with AHFS. However, it is invasive, and is associated with complications such as pneumothorax, infection, arrhythmias, and bleeding. Previous studies have suggested that this invasive procedure neither decreases risk of overall in-hospital mortality or length of stay, nor confers benefit in critically ill patients [32, 33]. By contrast, Doppler echocardiography is currently the primary clinical method for noninvasive measurement of hemodynamic parameters, and may obviate the need for invasive catheterization [16]. Numerous previous investigations have demonstrated that results of noninvasive Doppler techniques are highly reproducible and accurate in the assessment of RAP, pulmonary artery pressures, PCWP, and CO [20, 34, 35]. Third, we did not study the effects of intravenous administration of carperitide or nicorandil on symptoms. Furthermore, the end points used were not true end points such as morbidity and mortality, and were instead surrogate scales. Other limitations include a lack of an appropriate evidence-based titration regimen for carperitide or nicorandil. Because of these limitations, our results must be considered preliminary. Further well-designed, larger-scale studies would be useful for extending our findings to yield more practical guidelines for AHFS in settings closely resembling those of daily clinical practice.

Conclusions

Carperitide and nicorandil were differentially effective in improving hemodynamics in patients with AHFS. An improvement in estimated PCWP and urine output was greater in the carperitide group than in the nicorandil group, while an improvement in estimated CO was superior in the nicorandil group, suggesting a natriuretic action of carperitide and an arterial vasodilatory effect of nicorandil. Knowledge of these differences may enable physicians in emergency wards to treat and manage AHFS patients more effectively and safely.

Acknowledgments We thank Erisa Watanabe, Yuri Ozaki, and Keiko Hayashi for excellent clinical assistance, and Katsunori Shimada, PhD (STATZ Institute, Inc., Tokyo, Japan) for expert statistical assistance.

Conflict of interest None.

References

1. Gheorghiade M, Pang PS (2009) Acute heart failure syndromes. J Am Coll Cardiol 53:557–573
2. Gheorghiade M, Zannad F, Sopko G, Klein L, Pina IL, Konstam MA, Massie BM, Roland E, Targum S, Collins SP, Filippatos G, Tavazzi L (2005) Acute heart failure syndromes: current state and framework for future research. Circulation 112:3958–3968
3. Dickstein K, Cohen-Solal A, Filippatos G, McMurray JJ, Ponikowski P, Poole-Wilson PA, Stromberg A, van Veldhuisen DJ, Atar D, Hoes AW, Keren A, Mebazaa A, Nieminen M, Priori SG, Swedberg K (2008) ESC Guidelines for the diagnosis and treatment of acute and chronic heart failure 2008: the Task Force for the Diagnosis and Treatment of Acute and Chronic Heart Failure 2008 of the European Society of Cardiology. Developed in collaboration with the Heart Failure Association of the ESC (HFA) and endorsed by the European Society of Intensive Care Medicine (ESICM). Eur Heart J 29:2388–2442
4. Lee CY, Burnett JC Jr (2007) Natriuretic peptides and therapeutic applications. Heart Fail Rev 12:131–142
5. Saito Y, Nakao K, Nishimura K, Sugawara A, Okumura K, Obata K, Sonoda R, Ban T, Yasue H, Imura H (1987) Clinical application of atrial natriuretic polypeptide in patients with congestive heart failure: beneficial effects on left ventricular function. Circulation 76:115–124
6. Zhao Q, Wu TG, Lin Y, Li B, Luo JY, Wang LX (2010) Low-dose nesiritide improves renal function in heart failure patients following acute myocardial infarction. Heart Vessels 25:97–103

7. Nomura F, Kurobe N, Mori Y, Hikita A, Kawai M, Suwa M, Okutani Y (2008) Multicenter prospective investigation on efficacy and safety of carperitide as a first-line drug for acute heart failure syndrome with preserved blood pressure: COMPASS: carperitide effects observed through monitoring dyspnea in acute decompensated heart failure study. Circ J 72:1777–1786
8. Suwa M, Seino Y, Nomachi Y, Matsuki S, Funahashi K (2005) Multicenter prospective investigation on efficacy and safety of carperitide for acute heart failure in the 'real world' of therapy. Circ J 69:283–290
9. Taira N (1989) Nicorandil as a hybrid between nitrates and potassium channel activators. Am J Cardiol 63:18J–24J
10. Giles TD, Pina IL, Quiroz AC, Roffidal L, Zaleski R, Porter RS, Karalis DG, Mohrland JS, Wolf DL, Hearron AE (1992) Hemodynamic and neurohumoral responses to intravenous nicorandil in congestive heart failure in humans. J Cardiovasc Pharmacol 20:572–578
11. Minami Y, Nagashima M, Kajimoto K, Shiga T, Hagiwara N (2009) Acute efficacy and safety of intravenous administration of nicorandil in patients with acute heart failure syndromes: usefulness of noninvasive echocardiographic hemodynamic evaluation. J Cardiovasc Pharmacol 54:335–340
12. Nieminen MS, Harjola VP (2005) Definition and epidemiology of acute heart failure syndromes. Am J Cardiol 96:5G–10G
13. Koide K, Yoshikawa T, Nagatomo Y, Kohsaka S, Anzai T, Meguro T, Ogawa S (2010) Elevated troponin T on discharge predicts poor outcome of decompensated heart failure. Heart Vessels 25:217–222
14. Hata N, Seino Y, Tsutamoto T, Hiramitsu S, Kaneko N, Yoshikawa T, Yokoyama H, Tanaka K, Mizuno K, Nejima J, Kinoshita M (2008) Effects of carperitide on the long-term prognosis of patients with acute decompensated chronic heart failure: the PROTECT multicenter randomized controlled study. Circ J 72:1787–1793
15. Kircher BJ, Himelman RB, Schiller NB (1990) Noninvasive estimation of right atrial pressure from the inspiratory collapse of the inferior vena cava. Am J Cardiol 66:493–496
16. Lee KS, Abbas AE, Khandheria BK, Lester SJ (2007) Echocardiographic assessment of right heart hemodynamic parameters. J Am Soc Echocardiogr 20:773–782
17. Yock PG, Popp RL (1984) Noninvasive estimation of right ventricular systolic pressure by Doppler ultrasound in patients with tricuspid regurgitation. Circulation 70:657–662
18. Lee RT, Lord CP, Plappert T, Sutton MS (1989) Prospective Doppler echocardiographic evaluation of pulmonary artery diastolic pressure in the medical intensive care unit. Am J Cardiol 64:1366–1370
19. Ihlen H, Amlie JP, Dale J, Forfang K, Nitter-Hauge S, Otterstad JE, Simonsen S, Myhre E (1984) Determination of cardiac output by Doppler echocardiography. Br Heart J 51:54–60
20. Stein JH, Neumann A, Preston LM, Costanzo MR, Parrillo JE, Johnson MR, Marcus RH (1997) Echocardiography for hemodynamic assessment of patients with advanced heart failure and potential heart transplant recipients. J Am Coll Cardiol 30:1765–1772
21. Shirakabe A, Hata N, Yokoyama S, Shinada T, Kobayashi N, Asai K, Mizuno K (2010) Efficacy and safety of nicorandil therapy in patients with acute heart failure. J Cardiol 56:339–347
22. Tanaka K, Kato K, Takano T, Katagiri T, Asanoi H, Nejima J, Nakashima M, Kamijo T, Sakanashi M (2010) Acute effects of intravenous nicorandil on hemodynamics in patients hospitalized with acute decompensated heart failure. J Cardiol 56:291–299
23. Kobatake R, Sato T, Fujiwara Y, Sunami H, Yoshioka R, Ikeda T, Saito H, Ujihira T (2011) Comparison of the effects of nitroprusside versus nicorandil on the slow/no-reflow phenomenon during coronary interventions for acute myocardial infarction. Heart Vessels 26:379–384
24. Kanagawa K, Matsuo H (1984) Purification and complete amino acid sequence of alpha-human atrial natriuretic polypeptide (alpha-hANP). Biochem Biophys Res Commun 118:131–139
25. Serizawa T, Hirata Y, Kohmoto O, Iizuka M, Matsuoka H, Sato H, Takahashi T, Mochizuki T, Ishii M, Sugimoto T (1988) Acute hemodynamic effects of alpha human atrial natriuretic polypeptide in patients with congestive heart failure. Jpn Heart J 29:143–149
26. Hayashi M, Tsutamoto T, Wada A, Maeda K, Mabuchi N, Tsutsui T, Horie H, Ohnishi M, Kinoshita M (2001) Intravenous atrial natriuretic peptide prevents left ventricular remodeling in patients with first anterior acute myocardial infarction. J Am Coll Cardiol 37:1820–1826
27. Kosuge M, Miyajima E, Kimura K, Ishikawa T, Tochikubo O, Ishii M (1998) Comparison of atrial natriuretic peptide versus nitroglycerin for reducing blood pressure in acute myocardial infarction. Am J Cardiol 81:781–784
28. Filippatos G, Zannad F (2007) An introduction to acute heart failure syndromes: definition and classification. Heart Fail Rev 12:87–90
29. Gheorghiade M, De Luca L, Fonarow GC, Filippatos G, Metra M, Francis GS (2005) Pathophysiologic targets in the early phase of acute heart failure syndromes. Am J Cardiol 96:11G–17G
30. Kajimoto K, Sashida Y, Minami Y, Yumino D, Kawarai H, Kasanuki H (2009) Systolic blood pressure at admission as a predictor of the response to initial carperitide therapy in patients hospitalized for acute decompensated heart failure with left ventricular systolic dysfunction. Cardiovasc Drugs Ther 23:481–488
31. Kajimoto K, Shimamura K (2011) Acute efficacy of combined therapy of carperitide and nicorandil for acute decompensated heart failure with left ventricular systolic dysfunction. Int J Cardiol 149:e55–e58
32. Binanay C, Califf RM, Hasselblad V, O'Connor CM, Shah MR, Sopko G, Stevenson LW, Francis GS, Leier CV, Miller LW (2005) Evaluation study of congestive heart failure and pulmonary artery catheterization effectiveness: the ESCAPE trial. JAMA 294:1625–1633
33. Shah MR, Hasselblad V, Stevenson LW, Binanay C, O'Connor CM, Sopko G, Califf RM (2005) Impact of the pulmonary artery catheter in critically ill patients: meta-analysis of randomized clinical trials. JAMA 294:1664–1670
34. Thohan V (2004) Prognostic implications of echocardiography in advanced heart failure. Curr Opin Cardiol 19:238–249
35. Weeks SG, Shapiro M, Foster E, Michaels AD (2008) Echocardiographic predictors of change in left ventricular diastolic pressure in heart failure patients receiving nesiritide. Echocardiography 25:849–855

A Novel Disease Gene for Brugada Syndrome

Sarcolemmal Membrane–Associated Protein Gene Mutations Impair Intracellular Trafficking of hNav1.5

Taisuke Ishikawa, DVM*; Akinori Sato, MD, PhD*; Cherisse A. Marcou, BA; David J. Tester, BS; Michael J. Ackerman, MD, PhD; Lia Crotti, MD, PhD; Peter J. Schwartz, MD; Young Keun On, MD; Jeong-Euy Park, MD; Kazufumi Nakamura, MD, PhD; Masayasu Hiraoka, MD, PhD; Kiyoshi Nakazawa, MD, PhD; Harumizu Sakurada, MD, PhD; Takuro Arimura, DVM, PhD; Naomasa Makita, MD, PhD; Akinori Kimura, MD, PhD

Background—Mutations in genes including *SCN5A* encoding the α-subunit of the cardiac sodium channel (hNav1.5) cause Brugada syndrome via altered function of cardiac ion channels, but more than two-thirds of Brugada syndrome remains pathogenetically elusive. T-tubules and sarcoplasmic reticulum are essential in excitation of cardiomyocytes, and sarcolemmal membrane-associated protein (SLMAP) is a protein of unknown function localizing at T-tubules and sarcoplasmic reticulum.

Methods and Results—We analyzed 190 unrelated Brugada syndrome patients for mutations in *SLMAP*. Two missense mutations, Val269Ile and Glu710Ala, were found in heterozygous state in 2 patients but were not found in healthy individuals. Membrane surface expression of hNav1.5 in the transfected cells was affected by the mutations, and silencing of mutant *SLMAP* by small interfering RNA rescued the surface expression of hNav1.5. Whole-cell patch-clamp recordings of hNav1.5-expressing cells transfected with mutant *SLMAP* confirmed the reduced hNav1.5 current.

Conclusions—The mutations in *SLMAP* may cause Brugada syndrome via modulating the intracellular trafficking of hNav1.5 channel. (***Circ Arrhythm Electrophysiol.* 2012;5:1098-1107.**)

Key Words: arrhythmia mechanisms ■ genes ■ ion channels ■ sarcoplasmic reticulum

Brugada syndrome (BrS) is a cardiac channelopathy characterized by specific findings in the ECG such as accentuated J-wave and ST-segment elevation in the right precordial leads, which is often accompanied by syncope and sudden cardiac death attributable to ventricular arrhythmias.[1,2] Worldwide prevalence of BrS is ≈1 in 10 000, but it is much higher in Asian countries, reaching 5 to 10 in 10 000.[3–5] Approximately one-third of BrS patients have a family history of BrS and sudden cardiac death, which is consistent with the autosomal-dominant inheritance, suggesting that genetic abnormalities cause BrS.[6]

Clinical Perspective on p 1107

Mutations in 12 different genes have been reported in BrS.[7–13] The major disease gene for BrS is *SCN5A* that encodes the pore-forming α-subunit of the cardiac sodium channel hNav1.5; the *SCN5A* mutations reduce the availability of sodium channels, leading to the diminished peak of inward sodium current (I_{Na}) and the voltage-dependent shift in activation or inactivation profile attributable to the structural changes in the channel molecule or from trafficking abnormalities.[14,15] Mutations in genes encoding auxiliary

Received December 16, 2011; accepted September 13, 2012.

From the Department of Molecular Pathogenesis, Medical Research Institute, Tokyo Medical and Dental University, Tokyo, Japan (T.I., A.S., T.A., A.K.); Division of Cardiology, Niigata University Graduate School of Medical and Dental Sciences, Niigata, Japan (A.S.); Departments of Medicine (Division of Cardiovascular Diseases), Pediatrics (Division of Pediatric Cardiology), and Molecular Pharmacology and Experimental Therapeutics, Windland Smith Rice Sudden Death Genomics Laboratory, Mayo Clinic, Rochester, MN (C.A.M., D.J.T., M.J.A.); Institute of Human Genetics, Helmholtz Center Munich, Neuherberg, Germany (L.C.); Department of Molecular Medicine, Section of Cardiology, University of Pavia, Pavia, Italy (L.C., P.J.S.); Department of Cardiology, Fondazione IRCCS Policlinico S. Matteo, Pavia, Italy (L.C., P.J.S.); Cardiovascular Genetics Laboratory, Hatter Institute for Cardiovascular Research, Department of Medicine, University of Cape Town, Cape Town, South Africa (P.J.S.); Department of Medicine, University of Stellenbosch, Stellenbosch, South Africa (P.J.S.); Chair of Sudden Death, Department of Family and Community Medicine, College of Medicine, King Saud University, Riyadh, Saudi Arabia (P.J.S.); Division of Cardiology, Samsung Medical Center, Sungkyunkwan University School of Medicine, Seoul, Korea (Y.K.); Department of Cardiovascular Medicine, Okayama University Graduate School of Medicine, Dentistry and Pharmaceutical Sciences, Okayama, Japan (K.N.); Department of Cardiovascular Medicine, Medical Research Institute, Tokyo Medical and Dental University, Tokyo, Japan (M.H.); Division of Internal Medicine, Asao General Hospital, Kawasaki, Japan (K.N.); Department of Cardiology, Tokyo Metropolitan Hiroo Hospital, Tokyo, Japan (H.S.); and Department of Molecular Pathophysiology, Nagasaki University Graduate School of Biomedical Sciences, Nagasaki, Japan (N.M.).

The online-only Data Supplement is available at http://circep.ahajournals.org/lookup/suppl/doi:10.1161/CIRCEP.111.969972/-/DC1.

*These authors shared first authorship.

Correspondence to Akinori Kimura, MD, PhD, Department of Molecular Pathogenesis, Medical Research Institute, Tokyo Medical and Dental University, 1-5-45 Yushima, Bunkyo-ku, Tokyo 113–8510, Japan (e-mail akitis@tmd.ac.j); or Naomasa Makita, MD, PhD, Department of Molecular Pathophysiology, Nagasaki University Graduate School of Biomedical Sciences, 1-12-4 Sakamoto, Nagasaki 852-8523, Japan (e-mail: makitan@nagasaki-u.ac.jp).

Circ Arrhythm Electrophysiol **is available at http://circep.ahajournals.org** **DOI: 10.1161/CIRCEP.111.969972**

proteins regulating sodium channel function, such as glycerol-3-phosphate dehydrogenase-1–like enzyme and small subunits of sodium channel (hNavβ1 and hNavβ3) also are associated with BrS and the loss of hNav1.5 function.[16–18]

Excitation–contraction coupling is indispensable for the excitation of cardiomyocytes and is regulated by the functional association of T-tubules and sarcoplasmic reticulum.[19] It has been reported that abnormalities of T-tubules or sarcoplasmic reticulum can cause ventricular arrhythmias.[20–22] One of the components of T-tubules and sarcoplasmic reticulum is sarcolemmal membrane–associated protein (SLMAP), of which the gene *SLMAP* maps to chromosome 3p14.3–21.2 and encodes several isoforms of SLMAP via alternative splicing.[23] SLMAP is composed of several functional domains, including a forkhead-associated domain, a RecN domain, 2 leucine zipper domains, and a tail-anchor domain that is expressed as a mutually exclusive TM1 or TM2 domain. The tail-anchor domains play a pivotal role in subcellular targeting of SLMAP.[24] It is known that a ubiquitously expressed isoform, SLMAP3, is encoded by an open reading frame from the start codon in exon 1, whereas the other isoforms, SLMAP1 and SLMAP2, expressed abundantly in striated muscles including heart, are encoded by the other overlapping reading frames from different start codons.[25] Although the functional involvement of SLMAP in cardiac pathophysiology is largely unknown, SLMAP is a candidate gene to search for mutations in arrhythmias including BrS of unknownetiology.

In this study, we analyzed BrS patients for *SLMAP* mutations and investigated the functional significance of the identified mutations. The disease-associated *SLMAP* mutations decreased the cell surface expression of hNav1.5 and reduced the I_{Na} in transfected cells. This is the first report demonstrating the functional association of SLMAP with hNav1.5 and a novel pathogenic substrate for BrS.

Materials and Methods

Subjects

We studied 190 genetically unrelated patients with BrS. All patients manifested with a BrS diagnostic ECG pattern and were all free from mutations in *SCN5A* (BrS1).[26] Control subjects were 94 to 380 ethnic-matched healthy individuals. Blood sample was obtained from each subject after an informed consent for gene analysis was given. Data from public available databases as the 1000 genome project (http://www.1000genomes.org/) also were analyzed as controls. The research protocol was approved by the Ethics Review Committee of Medical Research Institute, Tokyo Medical and Dental University, the Mayo Foundation Institutional Review Board, and the Medical Ethical Committee of Fondazione IRCCS Policlinico San Matteo.

Mutational Analysis of SLMAP in BrS

Genomic DNA extracted from peripheral blood leukocytes of each individual was subjected to polymerase chain reaction using primer pairs for *SLMAP* (online-only Data Supplement Table I). Polymerase chain reaction products from Japanese patients were analyzed by direct sequencing method, whereas those from white patients underwent denaturing high-performance liquid chromatography and direct sequencing.[27] The sequencing of polymerase chain reaction products was performed using Big Dye Terminator version 3.1 (Applied Biosystems) and ABI3100 DNA analyzer (Applied Biosystems). The patients carrying rare nonsynonymous variations also were analyzed for mutations in all known BrS susceptibility genes (online-only Data Supplement Table II).

Constructs for SLMAP, hNavβ1, and hNav1.5

We obtained cDNA fragments for human SLMAP by reverse-transcription polymerase chain reaction from human heart cDNA. Wild-type (WT) cDNA fragment for SLMAP with TM1 or TM2 domain were amplified, and equivalent cDNA fragments containing a G-to-A substitution in codon 269 (for V269I), a C-to-A substitution in codon 288 (for H288Y), or an A-to-C substitution at codon 710 (for E710A) were created by the primer-mediated mutagenesis method (online-only Data Supplement Table III). The cDNA fragments of SLMAP were cloned into pEGFP-C1 for EGFP-SLMAP, pcDNA3.1 for pcDNA3.1-SLMAP, and pIRES-CD8 for pIRES-CD8-SLMAP. A cDNA fragment of hNavβ1 was cloned into pcDNA3.1-myc, and into His-B to obtain myc, His-hNavβ1. The cDNA fragment of human *SCN5A* was a gift from Dr A.L. George (Vanderbilt University, Nashville, TN). A Flag-tagged hNav1.5 was constructed by inserting a Flag epitope (DYKDDDDK) into the extracellular linker 1 between S1 and S2 in D1 domain after the position of aa154 in the hNav1.5 construct (L1-Flag-hNav1.5).[28] All constructs were sequenced to ensure that no errors were introduced.

Immunofluorescence Microscopy

HEK293 or H9c2 cells were seeded onto culture slides (BD Biosciences); 24 hours later, L1-Flag-hNav1.5 plus each EGFP-SLMAP with or without pcDNA3.1-SLMAP were transfected. After 48 hours of the transfection, the cells were permeabilized and incubated with the primary rabbit anti-Flag polyclonal Ab (Sigma) and secondary Alexa fluor 568 goat anti-rabbit IgG (Molecular Probes). Images of cells were collected and analyzed with LSM510 laser-scanning microscope. To quantify membrane expression of hNav1.5, fluorescence intensity at the entire cell area and the plasma membrane region (2 μm) in the middle *xy* images of *z* series stack were measured, and the ratios of peripheral to total cell area fluorescence intensity (PTAFI) were calculated as described previously.[16] Analyses of labeled cells were performed using ImageJ software (National Institutes of Health).[29]

Silencing of Transfected SLMAP by Small Interfering RNA

Predesigned small interfering RNA (siRNA) for human SLMAP (siRNA ID: s15435) and nonsilencing siRNA as a negative control were purchased from Ambion. HEK293 cells were seeded onto poly-D-Lysine–coated dishes or slides. After 24 hours, the cells were cotransfected with the combination of EGFP-SLMAP and L1-Flag-hNav1.5 with the predesigned siRNA or nonsilencing siRNA. After 48 hours of the transfection, the cells were lysed and subjected to Western blot analyses.

Electrophysiological Studies

We used the tsA-201 cell line, a derivative of HEK293 cell line, in our electrophysiological study, as described previously.[28] In brief, the cells were transfected transiently with either WT or mutant EGFP-SLMAP or pIRES-CD8-SLMAP in combination with pcDNA3.1-Nav1.5. Sodium currents were recorded from the cells that were positive for EGFP or labeled with CD8-Dynabeads using the whole-cell patch-clamp techniques.

Statistical Analysis

Numerical data were expressed as means±SEM. The normal distributions and equal variances of the data in this study were confirmed by using Shapiro-Wilk test or *F* test, respectively. Statistical differences were analyzed using 1-way ANOVA followed by Dunnett test and Student *t* test. $P<0.05$ was considered to be statistically significant.

Table 1. Sequence Variations in Exons of SLMAP Found in Brugada Syndrome Patients and Controls

	Location in Exon	Position at Codon*	Nucleotide Change (Corresponding Amino Acid)	Asian BrS Patients† (n=88)	Japanese Controls (n=94–380)	White BrS Patients (n=102)	dbSNP
1	Exon 1	24	CTG (Leu) to CTA (Leu)	0	0 in 187	1	
2	Exon 1	31	GGC (Gly) to GGT (Gly)	1	3 in 187	0	
3	Exon 2	68	TAT (Tyr) to TTT (Phe)	6	3 in 174	0	
4	Exon 6	193	CTA (Leu) to CTG (Leu)	1	8 in 362	0	
5	Exon 7	217	TTA (Leu) to TTG (Leu)	3	4 in 269	0	rs74857771
6	Exon 8	269	GTT (Val) to ATT (Ile)	1	0 in 380	0	
7	Exon 9	288	CAT (His) to TAT (Tyr)	1	1 in 380	0	
8	Exon 14	408	GGG (Gly) to GGT (Gly)	1	3 in 180	0	
9	Exon 16	447	GAC (Asp) to GAT (Asp)	52	55 in 94	0	rs17058639
10	Exon 19	622	CTT (Leu) to CTA (Leu)	0	0 in 192	4	rs35219531
11	Exon 19	630	CAG (Gln) to CGG (Arg)	0	0 in 192	1	rs35029175
12	Exon 21	681	CAG (Gln) to CAA (Gln)	0	1 in 380	11	rs17745469
13	Exon 21	710	GAA (Glu) to GCA (Ala)	1	0 in 380	0	

BrS indicates Brugada syndrome; and SLMAP, sarcolemmal membrane–associated protein.
*Codon number is that for SLMAP3.
†Japanese patients (n=85) and Korean patients (n=3).

Results

Mutational Analysis of SLMAP

We analyzed 190 BrS patients for mutations in *SLMAP*, and 8 synonymous and 5 nonsynonymous genetic variants were detected (Table 1 and Figure 1A). Among them, 5 variants had been registered in a public database of polymorphisms the single nucleotide polymorphism database (dbSNP) database; Table 1). A nonsynonymous variant p.Tyr68Phe (c.203A>T) was a polymorphism found in both patients and controls at similar frequencies in the Japanese population. The other 4 synonymous variants were rare but may not be disease-causing mutations, because no functional impact was deduced.

Three other variants were identified in the heterozygous state in each patient, p.Val269Ile (c.805G>A), p.His288Tyr (c.862C>T), and p.Glu710Ala (c.2129A>C) (online-only Data Supplement Figure IA and Table 1). The p.Val269Ile and p.Glu710Ala missense mutations (V269I and E710A, respectively) were found in a 46-year-old male patient and in a 57-year-old male patient, respectively, who both experienced syncope and showed spontaneous saddle-back (V269I) or coved-type (E710A) ST elevation on ECG, whereas the p.His288Tyr variant (H288Y) was found in a 51-year-old male patient who had development of a diagnostic BrS pattern only after the infusion of class Ic drugs. ECG records of the patients with V269I or E710A showed no apparent conduction delay (Figure 1B and 1C, online-only Data Supplement Table IV). In addition, both of them did not show obvious cardiac structural and functional abnormalities. All these substitutions were predicted to affect evolutionary conserved residues of SLMAP (online-only Data Supplement Figure IB). Both V269I and H288Y should be expressed only in SLMAP3, whereas E710A would be expressed in all SLMAP isoforms (Figure 1A). Because these variants were found in Japanese patients, we analyzed 380 Japanese individuals selected at random. V269I and E710A were not detected in the controls, whereas H288Y was observed in 1 control (Table 1). In addition, V269I and E710A were absent among the 1094 individuals, descendants of various ancestries (381 European ancestry, 246 West African ancestry, 181 American ancestry, and 286 East Asian ancestry), whereas H288Y was reported in the 1000 genome project. The patients carrying these variants had no mutation in all the known BrS susceptibility genes and no family history of arrhythmia or sudden cardiac death. Family studies were not performed.

Decreased Cell Surface Expression of hNav1.5 in the Presence of Mutant SLMAPs

Because the majority of BrS-associated mutations are known to affect the hNav1.5 properties, including loss of cell surface expression, we tested whether the SLMAP mutations would affect the subcellular localization of hNav1.5. We examined expression of SLMAPs in cell lines available for transfection experiments and found the endogenous expression in HEK293, tsA-201, and H9c2 cells (online-only Data Supplement Figure II). We then analyzed the cell surface expression of hNav1.5 in HEK293 cells cotransfected with L1-Flag-hNav1.5 and EGFP-SLMAP3 or EGFP-SLMAP1 with the TM1 or TM2 domain (Figure 2). The PTAFI ratio of hNav1.5 in the cotransfected cells of L1-Flag-hNav1.5 and EGFP-SLMAP3-TM1-WT was similar to the PTAFI ratio in the transfectants of L1-Flag-hNav1.5 and EGFP-SLMAP3-TM2-WT. However, the PTAFI ratios in the transfected cells of L1-Flag-hNav1.5 with EGFP-SLMAP3-TM1-V269I, EGFP-SLMAP3-TM2-V269I, EGFP-SLMAP3-TM1-E710A, or EGFP-SLMAP3-TM2-E710A were significantly decreased, whereas the PTAFI ratios in the transfectants of L1-Flag-hNav1.5 with EGFP-SLMAP3-TM1-H288Y or EGFP-SLMAP3-TM2-H288Y were not significantly altered (Figure 2, online-only Data Supplement Table V). E710A in SLMAP3 also should be expressed as E261A in SLMAP1, and we found that the PTAFI ratios in the L1-Flag-hNav1.5 transfected cells of either EGFP-SLMAP1-TM1-E261A or EGFP-SLMAP1-TM2-E261A were significantly decreased.

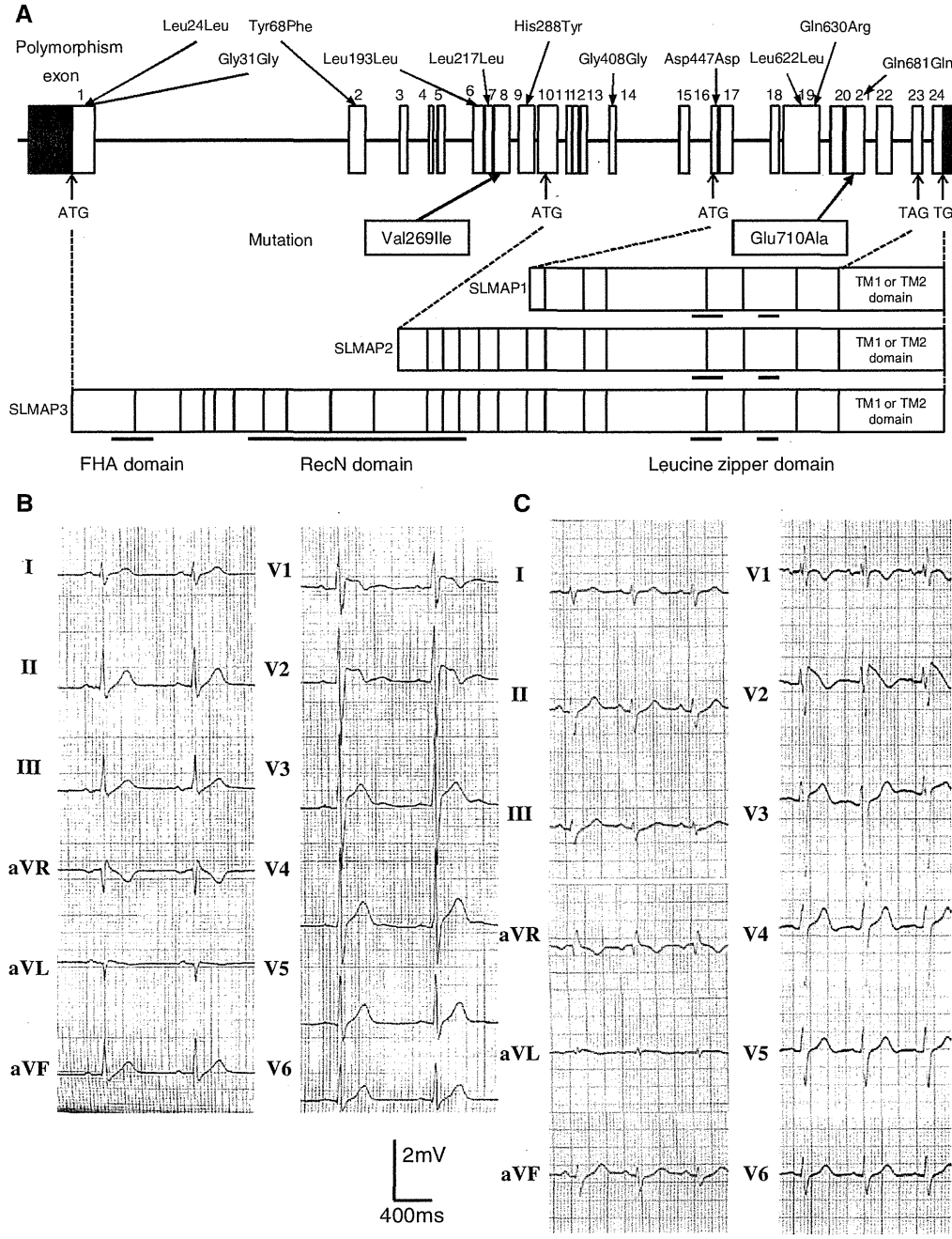

Figure 1. Mutational analysis of *SLMAP* gene in Brugada syndrome (BrS). **A**, Structure of *SLMAP* and sequence variations found in this study. **B** and **C**, Representative ECG records of the patients carrying V269I (**B**) or E710A (**C**). Both of them showed no apparent cardiac conduction delay.

To mimic a heterozygous state of *SLMAP* mutations, HEK293 cells were cotransfected with L1-Flag-hNav1.5, SLMAP3-TM1-WT, and each mutant SLMAP construct (Figure 3, online-only Data Supplement Table V). The PTAFI ratios in the L1-Flag-hNav1.5–transfected cells with both WT and mutant SLMAP were similar to those in the L1-Flag-hNav1.5–transfected cells with each mutant SLMAP, suggesting that V269I and E710A reduced the surface expression of hNav1.5 by a dominant-negative mechanism.

We also investigated the reduction of hNav1.5 expression by the *SLMAP* mutations in a rat cardiomyocyte–derived cell line, H9c2. H9c2 cells were transiently transfected with L1-Flag-hNav1.5 and either WT or mutant EGFP-SLMAP3-TM1. It was found that V269I and E710A mutations, but not H288Y, diminished the surface expression of hNav1.5 (online-only Data Supplement Figure III).

Silencing of Mutant SLMAPs Rescued the Cell Surface Expression of hNav1.5

To demonstrate the effect of *SLMAP* mutations on the surface expression of hNav1.5 by another method, we investigated whether silencing of the SLMAP mutants could rescue the decreased surface expression of hNav1.5. Silencing efficacy of predesigned siRNA for human *SLMAP* was evaluated, and it was

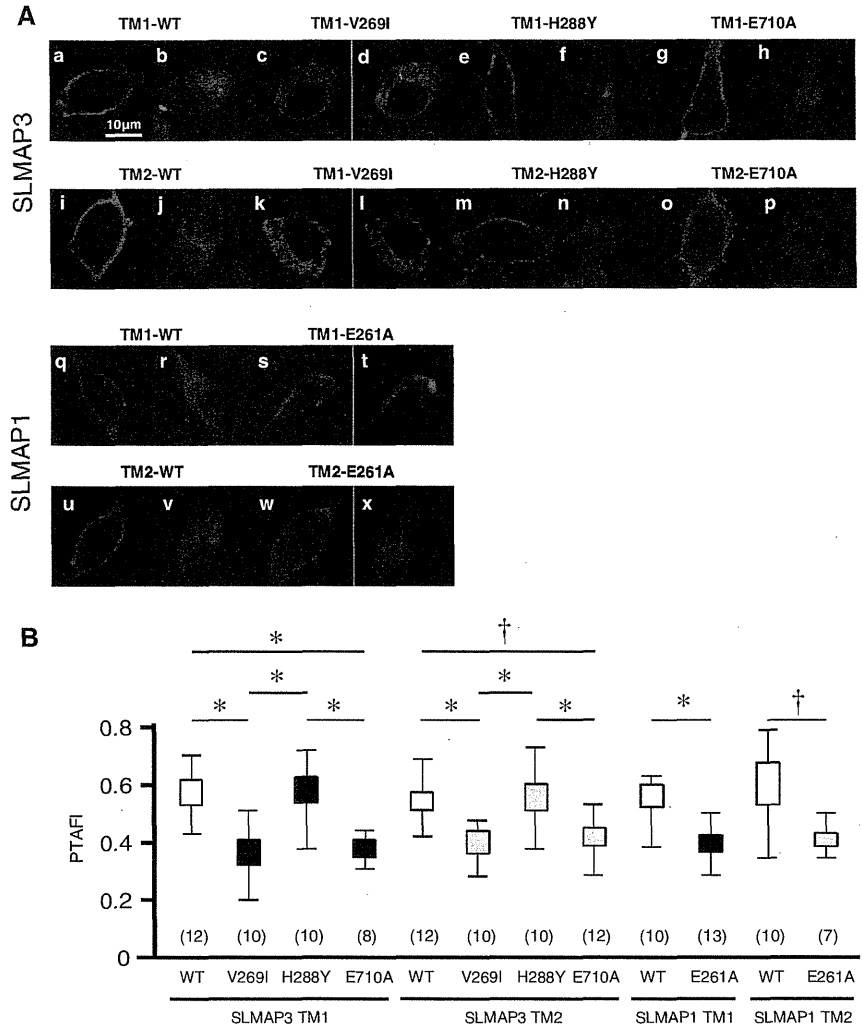

Figure 2. Fluorescence images of transiently expressed EGFP sarcolemmal membrane–associated protein (SLMAP) in HEK293 cells. **A**, Representative images of HEK293 cells cotransfected with L1-Flag-hNav1.5 and EGFP-SLMAP3-TM1-WT (**a** and **b**), EGFP-SLMAP3-TM1-V269I (**c** and **d**), EGFP-SLMAP3-TM1-H288Y (**e** and **f**), EGFP-SLMAP3-TM1-E710A (**g** and **h**), EGFP-SLMAP3-TM2-WT (**i** and **j**), EGFP-SLMAP3-TM2-V269I (**k** and **l**), EGFP-SLMAP3-TM2-H288Y (**m** and **n**), EGFP-SLMAP3-TM2-E710A (**o** and **p**), EGFP-SLMAP1-TM1-WT (**q** and **r**), EGFP-SLMAP1-TM1-E261A (**s** and **t**), EGFP-SLMAP1-TM2-WT (**u** and **v**), or EGFP-SLMAP1-TM2-E261A (**w** and **x**). The cells were permeabilized and stained with anti-Flag Ab (red; **a**, **c**, **e**, **g**, **i**, **k**, **m**, **o**, **q**, **s**, **u**, and **w**). Expression of EGFP-SLMAP is shown in **b**, **d**, **f**, **h**, **j**, **l**, **n**, **p**, **r**, **t**, **v**, and **x** (green). Scale bar, 10 μm. **B**, The ratio of peripheral to total cell area fluorescence intensity (PTAFI) of expressed L1-Flag-hNav1.5 in the transfected cells. Numbers of the analyzed cells are indicated at the bottom of each bar. *P<0.001; †P<0.01.

found that administration of siRNA at a final concentration of 30 nmol/L completely inhibited the SLMAP expression (Figure 4). HEK293 cells were transfected with the combinations of L1-Flag-hNav1.5, each EGFP-SLMAP construct, and predesigned siRNA to analyze the localization of hNav1.5.

The PTAFI ratios in the transfected cells of L1-Flag-hNav1.5 with each EGFP-SLMAP3 or EGFP-SLMAP1 were not changed in the presence of nonsilencing siRNA (Figure 4A). The PTAFI ratios in the cells expressing L1-Flag-hNav1.5 with EGFP-SLMAP3 of either WT or H288Y with the TM1 or TM2 domain were not significantly different between the presence of predesigned siRNA and nonsilencing siRNA (Figure 4B, online-only Data Supplement Table VI). However, the PTAFI ratios in the cells expressing L1-Flag-hNav1.5 with EGFP-SLMAP3-TM1-V269I or EGFP-SLMAP3-TM2-V269I were significantly higher in the presence of predesigned siRNA than in the presence of nonsilencing siRNA. Similarly, the ratios in the transfectants of L1-Flag-hNav1.5 with EGFP-SLMAP3-TM1-E710A or EGFP-SLMAP3-TM2-E710A were significantly higher in the presence of predesigned siRNA than in the presence of nonsilencing siRNA. The predesigned siRNA also could suppress the impaired surface expression of hNav1.5 caused by the E261A mutation in SLMAP1 (online-only Data Supplement Figure V and online-only Data Supplement Table V). The rescued expression levels, however, were similar to those in the L1-Flag-hNav1.5 transfected cells of EGFP-SLMAP1-WT with either predesigned siRNA or nonsilencing siRNA. These data indicated that the decreased surface expression of hNav1.5 was caused by the *SLMAP* mutations.

Altered Electrophysiological Characters Caused by the SLMAP Mutations

Because the impaired intracellular trafficking of hNav1.5 should result in the reduced hNav1.5 function, we investigated potential effects of the SLMAP mutants on the hNav1.5 kinetics. Whole-cell patch-clamp recordings were obtained from tsA-201 cells transiently transfected with pcDNA3.1-hNav1.5 in combination with EGFP-SLMAP3-WT or EGFP-SLMAP1-WT carrying either TM1 or TM2 domain. Peak current density of I_{Na} (pA/pF) recorded from the cells cotransfected with pcDNA3.1-hNav1.5 and EGFP-C1 was used as a control (Figure 5 and online-only Data Supplement Figures V and VI). It was found that the peak current densities recorded from the

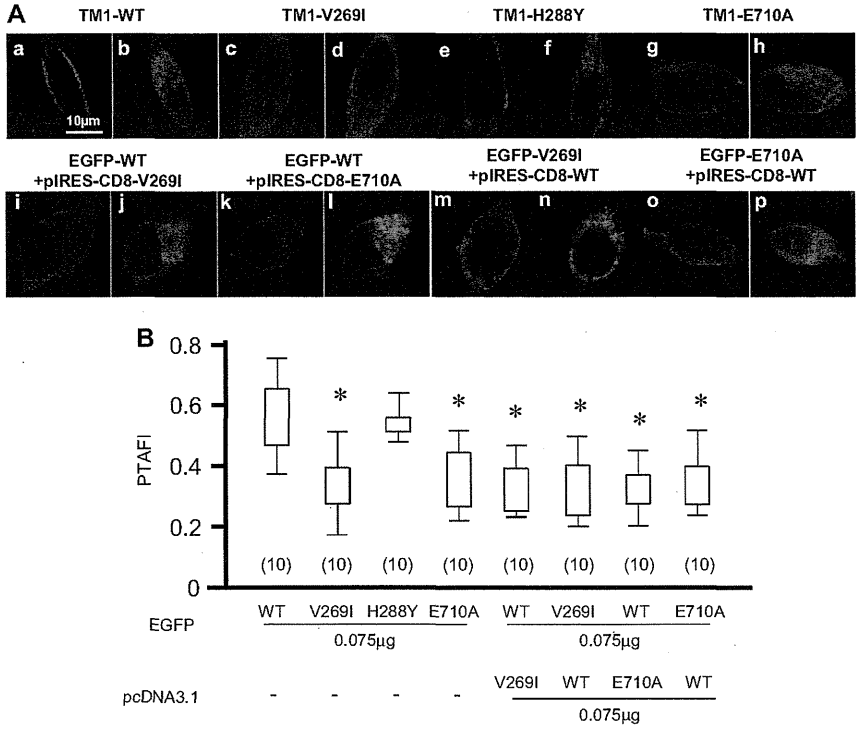

Figure 3. Fluorescence images of transiently expressed EGFP sarcolemmal membrane–associated protein (SLMAP) and pcDNA3.1-SLMAP in HEK293 cells. **A**, Representative images of HEK293 cells cotransfected with L1-Flag-hNav1.5 and EGFP-SLMAP3-TM1-WT (**a** and **b**), EGFP-V269I (**c** and **d**), EGFP-H288Y (**e** and **f**), EGFP-E710A (**g** and **h**), EGFP-WT plus pcDNA3.1-V269I (**i** and **j**), EGFP-V269I plus pcDNA3.1-WT (**k** and **l**), EGFP-WT plus pcDNA3.1-E710A (**m** and **n**), or EGFP-E710A plus pcDNA3.1-WT (**o** and **p**), The cells were permeabilized and stained with anti-Flag Ab (red; **a**, **c**, **e**, **g**, **i**, **k**, **m**, and **o**). Expression of EGFP-SLMAP is shown in **b**, **d**, **f**, **h**, **j**, **l**, **n**, and **p** (green). Scale bar, 10 μm. **B**, The ratio of peripheral to total cell area fluorescence intensity (PTAFI) of expressed L1-Flag-hNav1.5 in the transfected cells. Numbers of the analyzed cells are indicated at the bottom of each bar. *P<0.001.

transfected cells of pcDNA3.1-hNav1.5 with EGFP-SLMAP3 or EGFP-SLMAP1 in the TM1 or TM2 domain were not significantly different from that of the control. In addition, they did not show any significant changes in the activation and inactivation kinetics of I_{Na} and the time course of recovery from inactivation, as compared with EGFP only (Tables 2 and 3).

When we analyzed the effect of mutant SLMAP3 carrying V269I, H288Y, or E710A on the kinetics of hNav1.5 in the transfected cells (Figure 5, online-only Data Supplement Figure V), the peak current densities recorded from the cells cotransfected with pcDNA3.1-hNav1.5 and EGFP-SLMAP3-H288Y were similar to those recorded from the cells cotransfected with pcDNA3.1-hNav1.5 and EGFP-SLMAP3-WT. In clear contrast, the peak current densities of I_{Na} recorded from the cells cotransfected with pcDNA3.1-hNav1.5 and EGFP-SLMAP3-V269I with TM1 or TM2 domain were significantly smaller than those recorded from the cells cotransfected with pcDNA3.1-hNav1.5 and EGFP-SLMAP3-WT with the TM1 or TM2 domain by 56.5% and 51.9%, respectively (Tables 2 and 3). In addition, the peak current densities recorded from the cells cotransfected with pcDNA3.1-hNav1.5 and EGFP-SLMAP3-E710A with the TM1 or TM2 domain were significantly smaller than those recorded from the cells cotransfected with pcDNA3.1-hNav1.5 and EGFP-SLMAP3-WT with the TM1 or TM2 domain by 49.7% and 40.7%, respectively. However, none of the EGFP-SLMAP3-V269I, EGFP-SLMAP3-H288Y, and EGFP-SLMAP3-E710A caused significant changes in the activation and inactivation kinetics of I_{Na} and the time constants for recovery from inactivation.

We also investigated whether E261A mutation in SLMAP1 would show an effect on hNav1.5 kinetics as E710A mutation in SLMAP3 did. It was demonstrated that the peak current densities recorded from the cells cotransfected with pcDNA3.1-hNav1.5 and EGFP-SLMAP1-E261A were significantly lower than those recorded from the cells cotransfected with pcDNA3.1-hNav1.5 and EGFP-SLMAP1-WT by ≈40% without any significant changes in the activation and inactivation kinetics of I_{Na} and the time constants for recovery from inactivation (Tables 2 and 3, online-only Data Supplement Figure VI).

To exclude a possibility that the EGFP fused to SLMAP might affect the function of SLMAP or hNav1.5, we recorded I_{Na} from cells transiently transfected with pcDNA3.1-hNav1.5 and pIRES-CD8-SLMAP3 with or without mutation or variation (online-only Data Supplement Figure VII, online-only Data Supplement Table VII). It was observed that pIRES-CD8-SLMAP3-V269I and pIRES-CD8-SLMAP3-E710A decreased the peak current densities of I_{Na} to a similar extent as EGFP-fused SLMAPs. The effect of SLMAP mutations appeared to be exerted by a dominant-negative mechanism, as observed for the trafficking impairment.

Binding Between SLMAP and hNav1.5

Because the *SLMAP* mutations might modulate I_{Na} through a physical interaction with hNav1.5, we investigated whether SLMAP bound hNav1.5. No direct interaction between SLMAP and hNav1.5 was found under the condition in which the binding of hNav1.5 and hNavβ1 could be detected (online-only Data Supplement Figure VIII).

Discussion

Arrhythmias can be caused by mutations in the genes encoding ion channels producing action potentials.[30] In BrS, sodium current is more frequently affected than the other currents, such as calcium and potassium currents.[31] The affected sodium current is caused by mutations in the gene encoding hNav1.5, *SCN5A*, or genes for modifier proteins.[13,16–18] Prevalence of *SCN5A* mutations in BrS is ≈20%, whereas the prevalence of

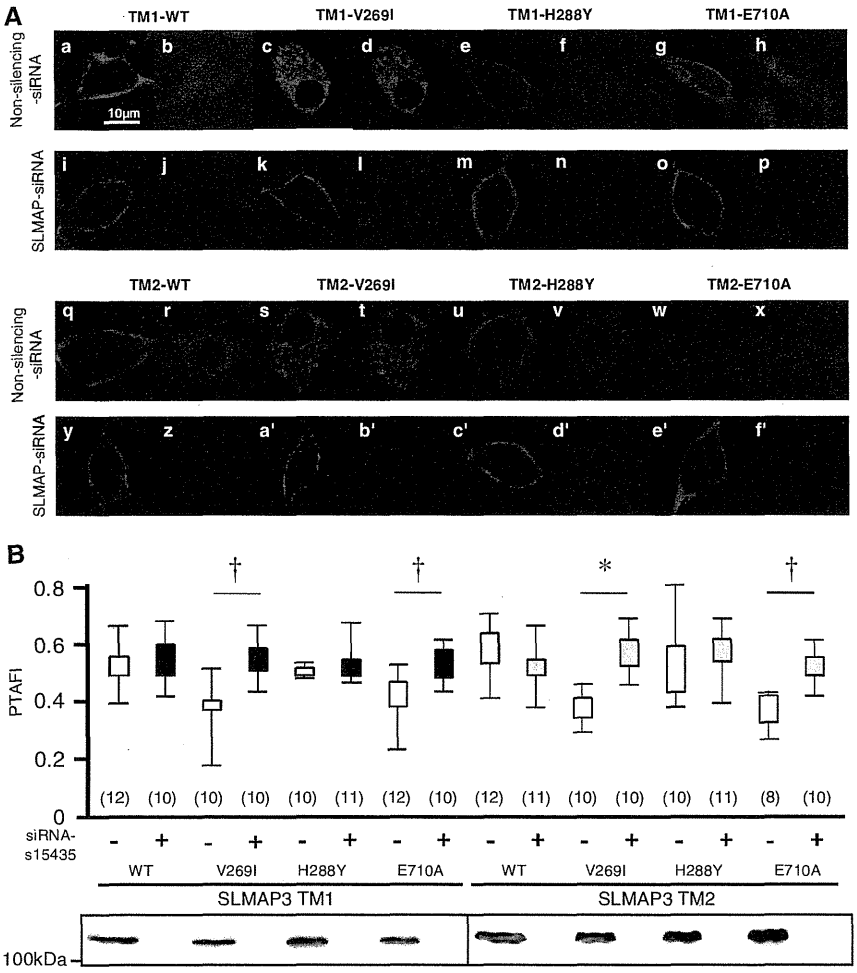

Figure 4. Silencing of transiently expressed *SLMAP3* in HEK293 cells. **A**, Representative images of HEK293 cells cotransfected with L1-Flag-hNav1.5 and EGFP sarcolemmal membrane–associated protein (SLMAP) 3-TM1-WT (**a**, **b**, **i** and **j**), EGFP-SLMAP3-TM1-V269I (**c**, **d**, **k**, and **l**), EGFP-SLMAP3-TM1-H288Y (**e**, **f**, **m** and **n**), EGFP-SLMAP3-TM1-E710A (**g**, **h**, **o**, and **p**), EGFP-SLMAP3-TM2-WT (**q**, **r**, **y**, and **z**), EGFP-SLMAP3-TM2-V269I (**s**, **t**, **a′**, and **b″**), EGFP-SLMAP3-TM2-H288Y (**u**, **v**, **c′**, and **d′**), or EGFP-SLMAP3-TM2-E710A (**w**, **x**, **e′**, and **f′**) in the presence of nonsilencing (**a–h** and **q–x**) or predesigned (**i–p** and **y–f′**) small interfering RNA (siRNA). The cells were permeabilized and stained with anti-Flag Ab (red; **a**, **c**, **e**, **g**, **i**, **k**, **m**, **o**, **q**, **s**, **u**, **w**, **y**, **a′**, **c′**, and **e′**). Expression of EGFP-SLMAP3 is shown in **b**, **d**, **f**, **h**, **j**, **l**, **n**, **p**, **r**, **t**, **v**, **x**, **z**, **b′**, **d′**, and **f′** (green). Scale bar, 10 μm. **B**, The ratio of peripheral to total cell area fluorescence intensity (PTAFI) of expressed L1-Flag-hNav1.5 in the transfected cells. Numbers of analyzed cells are indicated at the bottom of each bar. Silencing of EGFP-SLMAP3 by predesigned siRNA against human SLMAP (s15435) is shown in the **bottom**. PTAFIs were compared between the cells transfected with nonsilencing siRNA and with SLMAP-siRNA. **P*<0.001; †*P*<0.01; ‡*P*<0.05.

mutations in the other genes is relatively low.[31–34] In the present study, genetic analysis of *SLMAP* revealed a low prevalence of mutation, 2 in 190 BrS patients. Functional studies of the mutations suggested that SLMAP might be a modifier protein of hNav1.5 function. Because hNav1.5 and modifier proteins compose the sodium channel complex to generate and regulate the sodium current, functional abnormality of any components of the complex might alter the electrophysiological characters of cardiomyocytes.[30]

BrS-associated mutations in genes for the components of sodium channel complex usually result in loss of hNav1.5 function, including the voltage-dependent shift in the steady-state inactivation and activation profile, increased onset of inactivation, and decreased I_{Na}.[14] It was reported that mutations in the gene for hNavβ1, an auxiliary subunit of the sodium channel, affected the modulation of hNav1.5 channel gating.[17] Here, we demonstrate that the *SLMAP* mutations do not affect the voltage dependence in inactivation or activation profiles, suggesting that the mutations do not biophysically alter the hNav1.5 channel gating. However, the *SLMAP* mutations exerted a biogenic effect by reducing the surface expression of hNav1.5,

Table 2. Electrophysiological Properties of Transfected tsA-201 Cells of pcDNA3.1-hNav1.5 and Sarcolemmal Membrane–Associated Protein Constructs With Sarcolemmal Membrane–Associated Protein 3 Constructs

	WT-TM1	n	V269I-TM1	n	H288Y-TM1	n	E710A-TM1	n	WT-TM2	n	V269I-TM2	n	H288Y-TM2	n	E710A-TM2	n
Current density at −30 mV (pA/pF)	−336.2±63.6	11	−146.3±10.7*	9	−310.3±63.7	7	−169.2±15.7*	16	−373.2±45.9	13	−179.5±26.1*	11	−283.2±55.7	12	−221.4±40.6*	13
Voltage dependence of inactivation ($V_{1/2}$, mV)	−84.72±1.26	12	−86.13±0.98	9	−84.28±1.54	7	−84.47±1.15	15	−86.31±0.94	15	−86.32±0.79	13	−83.4±1.15	15	−85.36±1.37	15
Voltage dependence of activation ($V_{1/2}$, mV)	−46.40±1.85	8	−44.62±1.00	9	−47.46±1.72	7	−43.68±1.09	20	−47.07±1.25	13	−47.23±1.17	9	−45.51±1.59	12	−44.11±1.34	12
Time required for e^{-1} fraction recovery, ms	8.39±1.16	9	9.34±1.28	9	9.88±1.21	7	9.40±1.29	17	9.31±1.11	11	9.11±1.00	9	9.42±2.11	12	9.40±1.29	14

WT indicates wild-type.
**P*<0.05 vs WT.

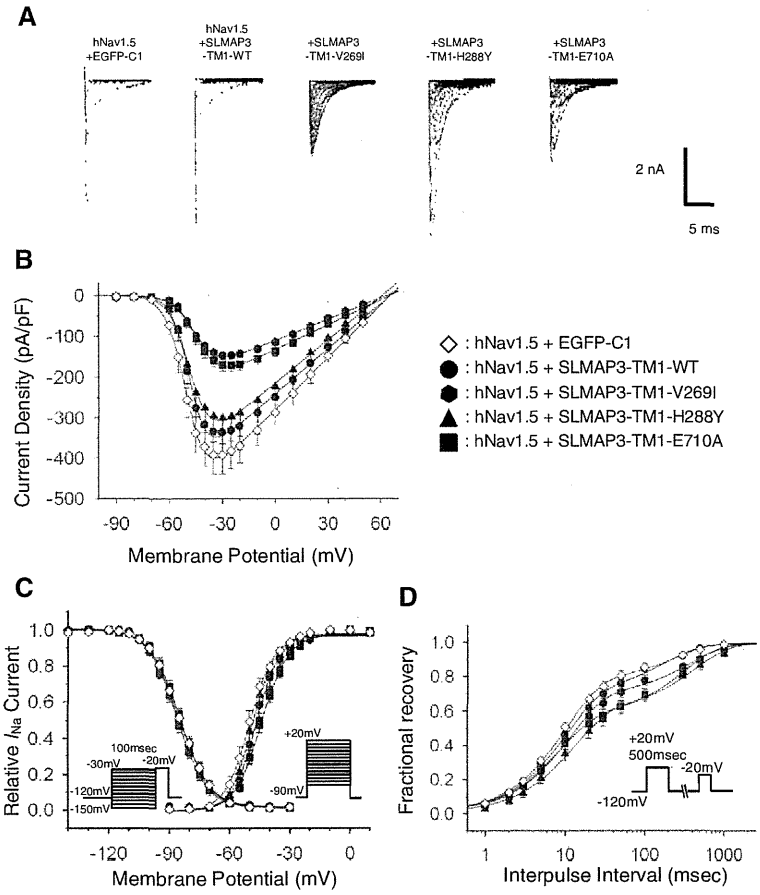

Figure 5. Sodium currents recorded from tsA-201 cells cotransfected with Nav1.5 and sarcolemmal membrane–associated protein (SLMAP) 3-TM1 constructs. **A**, Representative sodium currents were recorded from transfected tsA-201 cells of pcDNA3.1-hNav1.5 with EGFP, EGFP-SLMAP3-wild type (WT), EGFP-SLMAP3-V269I, EGFP-SLMAP3-H288Y, or EGFP-SLMAP3-E710A with TM1 domain. These traces were recorded with the whole-cell configuration as shown in the inset. **B**, Current–voltage relationship for peak I_{Na}. EGFP-SLMAP3-V269I and EGFP-SLMAP3-E710A showed a significant decline of peak current densities by 56.5% and 49.7% (n=11 for WT, n=9 for V269I, n=16 for E710A) at −30mV, whereas EGFP-SLMAP3-H288Y (n=7) did not alter the peak current density. **C**, The voltage dependence of steady-state fast inactivation and activation recorded from the transfected cells of pcDNA3.1-hNav1.5 in combination with EGFP, EGFP-SLMAP3-V269I, SLMAP3-H288Y, or EGFP-SLMAP3-E710A with TM1 domain were similar to that from the cells cotransfected with pcDNA3.1-hNav1.5 and EGFP-SLMAP3-WT with TM1 domain. **D**, Recovery from inactivation assessed by the double-pulse protocol was nearly identical among WT, V269I, H288Y, and E710A in SLMAP3. The 2-pulse protocol is shown in the inset.

culminating in decreased peak sodium current density and BrS susceptibility.

SLMAP is a member of tail-anchored proteins, which have a single TM domain at the C-terminal end to determine the subcellular localization. Tail-anchored proteins are involved in a variety of important cellular functions such as apoptosis, protein translocation, and membrane fusion in the organelles, where the proteins are anchored by the TM domain.[35] In the present study, we used SLMAPs carrying either the TM1 or TM2 domain and demonstrated that the mutation-related functional alteration could be observed similarly in any of the SLMAP isoforms with different TM domains, suggesting that the impaired hNav1.5 trafficking was attributable to the functional alterations of SLMAP in the endoplasmic reticulum, where SLMAP with either TM1 or TM2 domain could be localized.[24] Interestingly, SLMAP regulates the translocation of insulin-regulated glucose transporter GLUT4 from an intracellular compartment to the plasma membrane in adipose tissue, demonstrating the role of SLMAP in the intracellular trafficking.[36]

We showed that the SLMAP mutants impaired the surface expression of hNav1.5. However, no direct binding of hNav1.5 and SLMAP was detected in this study, speculating that SLMAP might indirectly contribute to the action potential in cardiomyocytes by modulating hNav1.5 localization. It has been demonstrated that MOG1 binds hNav1.5, and a MOG1 mutation causes BrS via an intracellular trafficking defect.[13] Then, the mechanism of impaired hNav1.5 trafficking caused by the SLMAP mutations was different from that caused by the MOG1 mutation. Recently, it was reported that a Z-disc protein, ZASP, formed a macromolecular

Table 3. Electrophysiological Properties of Transfected tsA-201 Cells of pcDNA3.1-hNav1.5 and Sarcolemmal Membrane–Associated Protein Constructs With Sarcolemmal Membrane–Associated Protein 1 Constructs and No Sarcolemmal Membrane–Associated Protein Control

	WT-TM1	n	E261A-TM1	n	WT-TM2	n	E261A-TM2	n	EGFP-C1	n
Current density at −30mV (pA/pF)	−413.6±52.6	8	−253.4±44.5†	14	−410.2±39.7	11	−246.6±26.7*	13	−394.0±65.8	15
Voltage dependence of inactivation ($V_{1/2}$, mV)	−86.61±1.29	9	−87.46±1.25	15	−80.46±1.19	12	−81.69±0.98	13	−83.25±1.41	15
Voltage dependence of activation ($V_{1/2}$, mV)	−49.29±2.14	8	−43.19±1.60	14	−45.99±1.28	11	−41.39±1.20	13	−49.83±1.99	15
Time required for e^{-1} fraction recovery (msec)	6.75±0.61	15	7.35±0.55	14	8.67±0.67	10	7.93±1.16	12	7.85±0.89	15

WT indicates wild-type.
*P<0.001.
†P<0.05 vs WT.

complex with hNav1.5, but there was no direct interaction between ZASP and hNav1.5, and a *ZASP* mutation disturbed the hNav1.5 function without affecting the localization of hNav1.5.[37] The function of hNav1.5 in cardiomyocytes may be regulated by a fine-tuning mechanism in which many proteins are directly or indirectly involved. Finally, although the loss of hNav1.5 function is often associated with prolongation of PR and QRS, no conduction delay was observed in ECGs from both patients carrying the *SLMAP* mutations. This might be attributable to the difference in severity of functional loss, or it might depend on the nature of affected genes. Further studies will be required to clarify the mechanisms causing the phenotypic difference in functional loss of hNav1.5.

In summary, we identified 2 *SLMAP* missense mutations associated with BrS, and the functional analyses indicated that mutant SLMAP biogenically impaired hNav1.5 trafficking. Like many of the BrS-associated auxiliary proteins, SLMAP-mediated BrS joins the most common pathogenic mechanism of BrS, sodium current loss-of-function BrS.

Sources of Funding

This work was supported in part by a grant-in-aid for Scientific Research from the Ministry of Education, Culture, Sports, Science, and Technology, Japan (22390157, 23132507, and 23659414 to A. Kimura, and 22136007 to N. Makita), Health and Labor Sciences research grant for research on measures of intractable diseases from the Ministry of Health, Labour, and Welfare, Japan (2010–119 to A. Kimura and 2010–145 to N. Makita), grants for Basic Scientific Cooperation Program between Japan and Korea from the Japan Society for the Promotion of Science (A. Kimura), National Research Foundation of Korea Grant (NRF-2010-E00024) (J-E. Park), a research grant from the Association Française contre les Myopathie (T. Arimura), Joint Usage/Research Program of Medical Research Institute Tokyo Medical and Dental University (A. Kimura), and the Windland Smith Rice Comprehensive Sudden Cardiac Death Program at the Mayo Clinic (M.J. Ackerman). This work also was supported by the follow-up grants provided from the Tokyo Medical and Dental University (A. Kimura).

Disclosures

M.J. Ackerman is a consultant for Transgenomic/FAMILION. Intellectual property derived from M.J. Ackerman's research program resulted in license agreements in 2004 between Mayo Clinic Health Solutions (formerly Mayo Medical Ventures) and PGxHealth (recently acquired by Transgenomic). The other authors have no conflicts to report.

References

1. Brugada P, Brugada J. Right bundle branch block, persistent ST segment elevation and sudden cardiac death: a distinct clinical and electrocardiographic syndrome. A multicenter report. *J Am Coll Cardiol.* 1992;20:1391–1396.
2. Chen PS, Priori SG. The Brugada syndrome. *J Am Coll Cardiol.* 2008;51:1176–1180.
3. Hermida JS, Lemoine JL, Aoun FB, Jarry G, Rey JL, Quiret JC. Prevalence of the brugada syndrome in an apparently healthy population. *Am J Cardiol.* 2000;86:91–94.
4. Miyasaka Y, Tsuji H, Yamada K, Tokunaga S, Saito D, Imuro Y, Matsumoto N, Iwasaka T. Prevalence and mortality of the Brugada-type electrocardiogram in one city in Japan. *J Am Coll Cardiol.* 2001;38:771–774.
5. Antzelevitch C, Brugada P, Borggrefe M, Brugada J, Brugada R, Corrado D, Gussak I, LeMarec H, Nademanee K, Perez Riera AR, Shimizu W, Schulze-Bahr E, Tan H, Wilde A. Brugada syndrome: report of the second consensus conference: endorsed by the Heart Rhythm Society and the European Heart Rhythm Association. *Circulation.* 2005;111:659–670.
6. Schulze-Bahr E, Eckardt L, Breithardt G, Seidl K, Wichter T, Wolpert C, Borggrefe M, Haverkamp W. Sodium channel gene (SCN5A) mutations in 44 index patients with Brugada syndrome: different incidences in familial and sporadic disease. *Hum Mutat.* 2003;21:651–652.
7. Kapplinger JD, Tester DJ, Alders M, Benito B, Berthet M, Brugada J, Brugada P, Fressart V, Guerchicoff A, Harris-Kerr C, Kamakura S, Kyndt F, Koopmann TT, Miyamoto Y, Pfeiffer R, Pollevick GD, Probst V, Zumhagen S, Vatta M, Towbin JA, Shimizu W, Schulze-Bahr E, Antzelevitch C, Salisbury BA, Guicheney P, Wilde AA, Brugada R, Schott JJ, Ackerman MJ. An international compendium of mutations in the SCN5A-encoded cardiac sodium channel in patients referred for Brugada syndrome genetic testing. *Heart Rhythm.* 2010;7:33–46.
8. Ueda K, Hirano Y, Higashiuesato Y, Aizawa Y, Hayashi T, Inagaki N, Tana T, Ohya Y, Takishita S, Muratani H, Hiraoka M, Kimura A. Role of HCN4 channel in preventing ventricular arrhythmia. *J Hum Genet.* 2009;54:115–121.
9. Medeiros-Domingo A, Tan BH, Crotti L, Tester DJ, Eckhardt L, Cuoretti A, Kroboth SL, Song C, Zhou Q, Kopp D, Schwartz PJ, Makielski JC, Ackerman MJ. Gain-of-function mutation S422L in the KCNJ8-encoded cardiac K(ATP) channel Kir6.1 as a pathogenic substrate for J-wave syndromes. *Heart Rhythm.* 2010;7:1466–1471.
10. Giudicessi JR, Ye D, Tester DJ, Crotti L, Mugione A, Nesterenko VV, Albertson RM, Antzelevitch C, Schwartz PJ, Ackerman MJ. Transient outward current (I(to)) gain-of-function mutations in the KCND3-encoded Kv4.3 potassium channel and Brugada syndrome. *Heart Rhythm.* 2011;8:1024–1032.
11. Burashnikov E, Pfeiffer R, Barajas-Martinez H, Delpón E, Hu D, Desai M, Borggrefe M, Häissaguerre M, Kanter R, Pollevick GD, Guerchicoff A, Laiño R, Marieb M, Nademanee K, Nam GB, Robles R, Schimpf R, Stapleton DD, Viskin S, Winters S, Wolpert C, Zimmern S, Veltmann C, Antzelevitch C. Mutations in the cardiac L-type calcium channel associated with inherited J-wave syndromes and sudden cardiac death. *Heart Rhythm.* 2010;7:1872–1882.
12. Amin AS, Tan HL, Wilde AA. Cardiac ion channels in health and disease. *Heart Rhythm.* 2010;7:117–126.
13. Kattygnarath D, Maugenre S, Neyroud N, Balse E, Ichai C, Denjoy I, Dilanian G, Martins RP, Fressart V, Berthet M, Schott JJ, Leenhardt A, Probst V, Le Marec H, Hainque B, Coulombe A, Hatem SN, Guicheney P. MOG1: a new susceptibility gene for Brugada syndrome. *Circ Cardiovasc Genet.* 2011;4:261–268.
14. Tfelt-Hansen J, Winkel BG, Grunnet M, Jespersen T. Inherited cardiac diseases caused by mutations in the Nav1.5 sodium channel. *J Cardiovasc Electrophysiol.* 2010;21:107–115.
15. Mohler PJ, Rivolta I, Napolitano C, LeMaillet G, Lambert S, Priori SG, Bennett V. Nav1.5 E1053K mutation causing Brugada syndrome blocks binding to ankyrin-G and expression of Nav1.5 on the surface of cardiomyocytes. *Proc Natl Acad Sci USA.* 2004;101:17533–17538.
16. Hu D, Barajas-Martinez H, Burashnikov E, Springer M, Wu Y, Varro A, Pfeiffer R, Koopmann TT, Cordeiro JM, Guerchicoff A, Pollevick GD, Antzelevitch C. A mutation in the beta 3 subunit of the cardiac sodium channel associated with Brugada ECG phenotype. *Circ Cardiovasc Genet.* 2009;2:270–278.
17. Watanabe H, Koopmann TT, Le Scouarnec S, Yang T, Ingram CR, Schott JJ, Demolombe S, Probst V, Anselme F, Escande D, Wiesfeld AC, Pfeufer A, Kääb S, Wichmann HE, Hasdemir C, Aizawa Y, Wilde AA, Roden DM, Bezzina CR. Sodium channel ß1 subunit mutations associated with Brugada syndrome and cardiac conduction disease in humans. *J Clin Invest.* 2008;118:2260–2268.
18. London B, Michalec M, Mehdi H, Zhu X, Kerchner L, Sanyal S, Viswanathan PC, Pfahnl AE, Shang LL, Madhusudanan M, Baty CJ, Lagana S, Aleong R, Gutmann R, Ackerman MJ, McNamara DM, Weiss R, Dudley SC Jr. Mutation in glycerol-3-phosphate dehydrogenase 1 like gene (GPD1-L) decreases cardiac Na+ current and causes inherited arrhythmias. *Circulation.* 2007;116:2260–2268.
19. Brette F, Orchard C. T-tubule function in mammalian cardiac myocytes. *Circ Res.* 2003;92:1182–1192.
20. Priori SG, Napolitano C, Tiso N, Memmi M, Vignati G, Bloise R, Sorrentino V, Danieli GA. Mutations in the cardiac ryanodine receptor gene (hRyR2) underlie catecholaminergic polymorphic ventricular tachycardia. *Circulation.* 2001;103:196–200.
21. Tiso N, Stephan DA, Nava A, Bagattin A, Devaney JM, Stanchi F, Larderet G, Brahmbhatt B, Brown K, Bauce B, Muriago M, Basso C, Thiene G,

Danieli GA, Rampazzo A. Identification of mutations in the cardiac ryanodine receptor gene in families affected with arrhythmogenic right ventricular cardiomyopathy type 2 (ARVD2). *Hum Mol Genet.* 2001;10:189–194.
22. Lahat H, Pras E, Olender T, Avidan N, Ben-Asher E, Man O, Levy-Nissenbaum E, Khoury A, Lorber A, Goldman B, Lancet D, Eldar M. A missense mutation in a highly conserved region of CASQ2 is associated with autosomal recessive catecholamine-induced polymorphic ventricular tachycardia in Bedouin families from Israel. *Am J Hum Genet.* 2001;69:1378–1384.
23. Guzzo RM, Sevinc S, Salih M, Tuana BS. A novel isoform of sarcolemmal membrane-associated protein (SLMAP) is a component of the microtubule organizing centre. *J Cell Sci.* 2004;117(Pt 11):2271–2281.
24. Byers JT, Guzzo RM, Salih M, Tuana BS. Hydrophobic profiles of the tail anchors in SLMAP dictate subcellular targeting. *BMC Cell Biol.* 2009;10:48.
25. Wigle JT, Demchyshyn L, Pratt MA, Staines WA, Salih M, Tuana BS. Molecular cloning, expression, and chromosomal assignment of sarcolemmal-associated proteins. A family of acidic amphipathic alpha-helical proteins associated with the membrane. *J Biol Chem.* 1997;272:32384–32394.
26. Benito B, Brugada R, Brugada J, Brugada P. Brugada syndrome. *Prog Cardiovasc Dis.* 2008;51:1–22.
27. Ackerman MJ, Tester DJ, Jones GS, Will ML, Burrow CR, Curran ME. Ethnic differences in cardiac potassium channel variants: implications for genetic susceptibility to sudden cardiac death and genetic testing for congenital long QT syndrome. *Mayo Clin Proc.* 2003;78:1479–1487.
28. Makita N, Behr E, Shimizu W, Horie M, Sunami A, Crotti L, Schulze-Bahr E, Fukuhara S, Mochizuki N, Makiyama T, Itoh H, Christiansen M, McKeown P, Miyamoto K, Kamakura S, Tsutsui H, Schwartz PJ, George AL Jr, Roden DM. The E1784K mutation in SCN5A is associated with mixed clinical phenotype of type 3 long QT syndrome. *J Clin Invest.* 2008;118:2219–2229.
29. Abramoff MD, Magelhaes PJ, Ram SJ. Processing with ImageJ. *Biophoton Int.* 2004;11:36–42.
30. Abriel H. Cardiac sodium channel Na(v)1.5 and interacting proteins: Physiology and pathophysiology. *J Mol Cell Cardiol.* 2010;48:2–11.
31. Hedley PL, Jørgensen P, Schlamowitz S, Moolman-Smook J, Kanters JK, Corfield VA, Christiansen M. The genetic basis of Brugada syndrome: a mutation update. *Hum Mutat.* 2009;30:1256–1266.
32. Eckardt L, Probst V, Smits JP, Bahr ES, Wolpert C, Schimpf R, Wichter T, Boisseau P, Heinecke A, Breithardt G, Borggrefe M, LeMarec H, Böcker D, Wilde AA. Long-term prognosis of individuals with right precordial ST-segment-elevation Brugada syndrome. *Circulation.* 2005;111:257–263.
33. Priori SG, Napolitano C, Gasparini M, Pappone C, Della Bella P, Giordano U, Bloise R, Giustetto C, De Nardis R, Grillo M, Ronchetti E, Faggiano G, Nastoli J. Natural history of Brugada syndrome: insights for risk stratification and management. *Circulation.* 2002;105:1342–1347.
34. Crotti L, Kellen CH, Tester D, Castelletti S, Giudessi JR, Torchio M, Medeiros-Domingo A, Savastano S, Will ML, Dagradi F, Schwartz PJ, Ackerman MJ. Spectrum and prevalence of mutations involving BrS1-12-susceptibility genes in a cohort of unrelated patients referred for Brugada syndrome genetic testing: implications for genetic testing. *J Am Col Cardiol.* 2012; 60:1410-1418.
35. Borgese N, Fasana E. Targeting pathways of C-tail-anchored proteins. *Biochim Biophys Acta.* 2011;1808:937–946.
36. Chen X, Ding H. Increased expression of the tail-anchored membrane protein SLMAP in adipose tissue from type 2 Tally Ho diabetic mice. *Exp Diabetes Res.* 2011;2011:421982.
37. Li Z, Ai T, Samani K, Xi Y, Tzeng HP, Xie M, Wu S, Ge S, Taylor MD, Dong JW, Cheng J, Ackerman MJ, Kimura A, Sinagra G, Brunelli L, Faulkner G, Vatta M. A ZASP missense mutation, S196L, leads to cytoskeletal and electrical abnormalities in a mouse model of cardiomyopathy. *Circ Arrhythm Electrophysiol.* 2010;3:646–656.

CLINICAL PERSPECTIVE

Brugada syndrome is an inherited channelopathy characterized by specific ECG findings and sometimes is associated with sudden cardiac arrest. Although the genetic causes of Brugada syndrome in the majority of the patients remain unknown, this disorder has been linked to mutations in the 12 different genes, which cause either a reduction of transient inward sodium or calcium current or an augmentation of transient outward potassium current. In particular, the sodium current is frequently affected because the majority of mutations were found in *SCN5A* encoding a large subunit of cardiac sodium channel hNav1.5. In addition to hNav1.5, auxiliary subunits, hNavβ1 and hNavβ3, and the proteins involved in trafficking, anchoring, or scaffolding of hNav1.5 are involved in propagating sodium current in cardiomyocytes, and mutations in the genes for these components could disturb sodium channel function and result in Brugada syndrome. The underlying molecular mechanisms for the disturbance of sodium channel are abnormalities in gating properties and trafficking efficacy. In this study, we identified the thirteenth disease gene, ie, we revealed that the mutations in *SLMAP* encoding for sarcolemmal membrane–associated protein, a sarcolemmal protein of unknown function, caused Brugada syndrome via a trafficking abnormality of the sodium channel. Our observations deciphered the physiological involvement of sarcolemmal membrane–associated protein in the fine-tuning of electrical propagation in cardiomyocytes and suggest that understanding the trafficking mechanisms of the sodium channel will clarify the pathogenesis of Brugada syndrome to develop a novel therapeutic strategy for Brugada syndrome.

Advance Publication by-J-STAGE

Circulation Journal
Official Journal of the Japanese Circulation Society
http://www.j-circ.or.jp

REVIEW

Tenascin-C in Cardiovascular Tissue Remodeling

– From Development to Inflammation and Repair –

Kyoko Imanaka-Yoshida, MD, PhD

Tenascin-C (TN-C) is a matricellular protein expressed during embryonic development, as well as in wound healing and cancer invasion in various tissues, and may regulate cell behavior and matrix organization during tissue remodeling. In the cardiovascular system, TN-C is transiently expressed at several important steps of embryonic development, playing important roles in the differentiation of cardiomyocytes and in coronary vasculo/angiogenesis. TN-C is sparse in normal adults, but upregulated under pathological conditions such as myocarditis, myocardial infarction, cardiac fibrosis, atherosclerosis, stenotic neointimal hyperplasia, and aneurysm, and is closely associated with tissue injury and inflammation. In view of its specific expression, TN-C could be a realistic and promising biomarker and a target for molecular imaging for the diagnosis of various cardiovascular diseases. TN-C also has diverse functions, including weakening of cell adhesion, up-regulating the expression and activity of matrix metalloproteinases, modulating inflammatory responses, promoting recruitment of myofibroblasts, and enhancing fibrosis. TN-C could exert both harmful and protective effects and might be a therapeutic target as a key molecule in the control of the balance of beneficial and undesirable cellular responses during tissue remodeling. (*Circ J* 2012; **76:** 2513–2520)

Key Words: Biomarker; Inflammation; Molecular imaging; Remodeling; Tenascin-C

Extracellular matrix (ECM) components are important for mechanical support and effective functioning of the cardiovascular system. Therefore, alteration of the ECM may directly result in changes of mechanical properties and functional impairment. The ECM also plays significant roles in tissue remodeling in stress responses. Among the ECM components, increased attention has been focused on the matricellular proteins, which are a growing group of non-structural ECM proteins with different structures but common unique properties: (1) high levels of expression during embryonic development and in response to injury; (2) binding to many cell-surface receptors, components of ECM, growth factors, cytokines, and proteases; and (3) induction of de-adhesion or counter-adhesion.[1,2] This group originally included thrombospondin-1,-2, osteonectin/SPARC, tenascin-C (TN-C), tenascin-X, osteopontin, and CCN (CY61/CTGF/NOV). Recently, new members such as periostin and galectin have joined the group. Matricellular proteins play a significant role in cardiovascular disease.[3–6] This review will focus on the role of TN-C, a typical matricellular protein, in cardiovascular development and disease.

TN-C

TN-C is a huge glycoprotein of approximately 300 kDa as an intact monomer, which is assembled into a hexamer.[7,8] Multiple cell-surface receptors, including integrins $\alpha 9\beta 1$, $\alpha v\beta 3$, and $\alpha v\beta 6$, and toll-like receptor 4 (TLR-4), bind to the respective domains of TN-C and transmit multiple signals that could control the balance of cell adhesion and de-adhesion, cell motility, proliferation, differentiation, and survival.[9,10]

TN-C is expressed transiently at specific sites during embryonic development, wound healing, cancer invasion, and regeneration, at locations where the tissue structure is being dynamically remodeled.[6,8,11,12] The expression of TN-C can be activated by a number of different stimuli, including cytokine growth factors and mechanical strain through multiple signaling pathways including nuclear factor κ B (NF-κB) and mitogen-activated protein kinase.[13] Several factors including miRNA-335[14,15] may directly suppress its gene activation, which should be important for the strict regulation of its expression.

TN-C knockout (TN-C KO) mice were initially reported to undergo normal development and have a normal life span and fertility without distinct phenotypes.[16,17] Recently, more detailed investigations have shown several differences in lung[18] and prostate[19] development in TN-C KO. Furthermore, evident differences have been reported in various disease models using TN-C KO, for example, attenuation of fibrotic/inflammatory lesions of various organs, including the cardiovascular system.[20–26]

Received August 10, 2012; revised manuscript received September 10, 2012; accepted September 13, 2012; released online October 13, 2012

Department of Pathology and Matrix Biology, Mie University Graduate School of Medicine, Tsu; Mie University Research Center for Matrix Biology, Tsu, Japan

Mailing address: Kyoko Imanaka-Yoshida, MD, PhD, Department of Pathology and Matrix Biology, Mie University Graduate School of Medicine, Tsu 514-8507, Japan. E-mail: imanaka@doc.medic.mie-u.ac.jp

ISSN-1346-9843 doi:10.1253/circj.CJ-12-1033

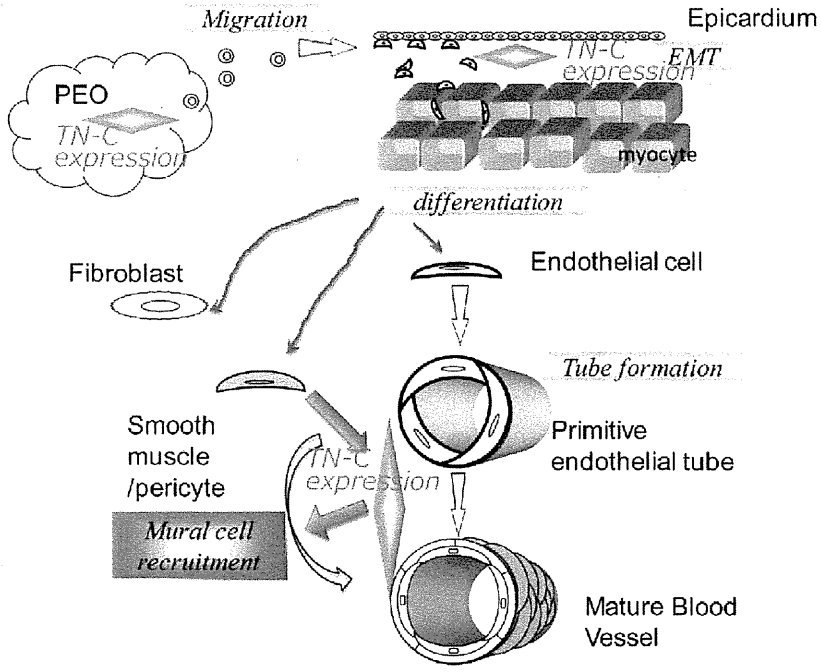

Figure 1. Schematic of coronary vasculogenesis and tenascin-C (TN-C) expression. EMT, epithelial-mesenchymal transition; PEO, proepicardial organ.

TN-C in the Heart

Heart Development and TN-C

During heart development, TN-C is transiently expressed at restricted sites at several important steps of heart morphogenesis:[27] (1) differentiation of cardiomyocytes, (2) cushion tissue and valve formation, and (3) coronary vessel formation.

It is particularly intriguing that the expression of TN-C appears to be closely related to cardiomyocyte differentiation. In the case of mice, the mesodermal cells from the cardiac crescent, called primary heart field or first heart field (FHF), differentiate to cardiomyocytes and endocardial cells at embryonic day 7.5. TN-C is expressed by the differentiating precardiac cells. Once the cells differentiate to cardiomyocytes, they rapidly stop expressing TN-C.[27] TN-C expression is also detected at the recruitment of the precardiac cells from the second heart field (SHF). In contrast to the FHF-derived cells, the cardiomyocytes from the SHF in the outflow tract maintain the expression of TN-C during looping and shortening.

Another important possibility is that TN-C may play a role in coronary vessel development. The progenitor of the coronary vascular system comes from the proepicardial organ (PEO), a cauliflower-like projection of transverse septum between the primitive heart and the liver bud. Mesenchymal cells from the PEO migrate to the primitive heart at embryonic day 9.5. They eventually form epicardium, undergo epithelial-mesenchymal transition (EMT), and give rise to vascular endothelial cells, smooth muscle cells, and cardiac fibroblasts.[28,29] TN-C is expressed in the PEO before the cells start to migrate and at epicardial EMT (Figure 1). TN-C is also expressed upon the maturation of coronary vessels and may promote the recruitment of α-smooth muscle actin (SMA)-positive mural cells to the primitive endothelial tubes by facilitating platelet-derived growth factor (PDGF)-BB/PDGFRβ signaling via integrin $\alpha v\beta 3$.[30,31]

Regardless of the potential roles during heart development predicted on the basis of spatiotemporal-restricted expression, hearts develop normally in TN-C knockout mice.[16,17,27] Furthermore, our recent preliminary data suggested that overexpression of TN-C in heart may not cause a distinct phenotype, either (unpublished data). Evidently, a compensatory mechanism should be present, which has not been identified yet.

Myocardial Injury, Inflammation in the Adult Heart, and TN-C

TN-C is sparsely detected in the normal adult myocardium, but reappears when the heart remodels its structure in response to pathologic insults, such as acute myocardial infarction (MI),[32–35] myocarditis,[36–38] hibernation,[39] ischemia-reperfusion,[40] hypertensive cardiac fibrosis,[41] chronic cardiac rejection[42] and some cases of dilated cardiomyopathy (DCM)[43,44] closely associated with inflammation.

Under these pathological conditions, myocardial cell death caused by destructive stress triggers inflammation, which is an important process for proper tissue repair. Accumulating evidence suggests that TN-C may enhance inflammatory responses.[25] For example, TN-C may activate innate immunity as DAMP (damage-associated molecular patterns) to stimulate the production of the proinflammatory cytokines in macrophages and fibroblasts via a TLR-4-mediated signaling pathway.[25,45] It also modulates adaptive immunity via the integrin $\alpha 9$ pathway[13,46] and cytokine upregulation[24] with the activation of NF-$\kappa\beta$.[23]

Tissue Repair After Acute MI

Tissue repair after MI is a typical example of wound healing followed by scar formation. Necrosis of myocytes elicits acute inflammation to remove dead cells and matrix debris. Then, activated interstitial cells form capillary-rich granulation tissue, remodel ECM, and finally replace myocardial dropout

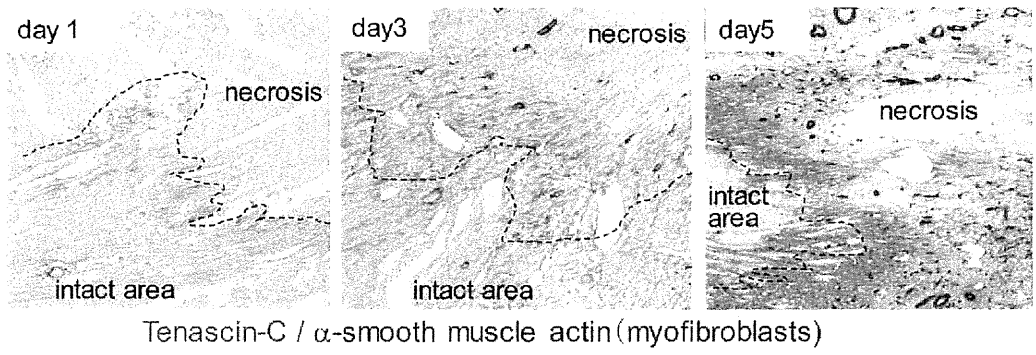

Figure 2. Distribution of myofibroblasts (blue) and tenascin-C (TN-C, brown) in histological sections from a myocardial infarction rat model. Dotted lines show the border line. (Adapted from Imanaka-Yoshida et al.[33])

with mature collagen fibers.[47,48]

TN-C is expressed during inflammation and granulation formation. It is striking that TN-C is exclusively localized at the border zone between residual myocardium and infarcted lesion.[20,26,33]

Several roles of TN-C during tissue repair after MI have been proposed.

First, TN-C could help tissue reconstruction of the edge of the residual myocardium as a "de-adhesion" protein. TN-C could loosen strong adhesion of cardiomyocytes[33,49] and up-regulate the expression and activity of matrix metalloproteinases (MMPs),[50] so that it may release surviving cardiomyocytes to reorganize their shape and arrangement. Concomitantly, TN-C may maintain weak attachment of the cardiomyocytes[33,49] and protect against anoikis. The elastic property of the TN-C molecule also suggests that it may act as a molecular dampener to protect the cells from destructive mechanical stress.[51] Moreover, a recent paper reported a significant role of TN-C in the regeneration of cardiomyocytes in zebra fish.[52]

In mammals, a major player in myocardial repair is the interstitial cells, because of the limited ability for the regeneration of cardiomyocytes. It is considered that fibroblastic cells recruited from different sources become protomyofibroblasts, move from the peri-infarcted area into the damaged lesion, and differentiate to α-SMA-positive myofibroblasts. Myofibroblasts play a central role in wound healing by synthesizing collagens and exerting strong contractile forces to promote wound healing.[53]

During myocardial tissue repair, the major source of TN-C is the interstitial fibroblasts in the vicinity of the injured cardiomyocytes, but cardiomyocytes themselves do not synthesize TN-C.[33,36,38] Initially, α-SMA-negative interstitial cells in the border zones express TN-C, and then α-SMA-positive myofibroblasts appear in the TN-C-positive areas (**Figure 2**). In vitro, TN-C facilitates the migration and expression of α-SMA of cardiac fibroblasts.[20] Furthermore, the appearance of myofibroblasts in the injured sites is delayed in TN-C KO.[20] Therefore, it is suggested that TN-C synthesized by interstitial cells at an early phase induces differentiation to myofibroblasts and promotes migration into damaged areas in an autocrine and paracrine fashion.

Moreover, TN-C may regulate angiogenesis, another important element of myocardial repair. In addition to the potential to facilitate coronary vasculogenesis in the embryo,[30] it may promote postnatal neovascularization by regulating bone marrow-derived endothelial progenitor cell homing and/or incorporation at sites of angiogenic induction, as well as local endothelial function.[54]

Cardiac Fibrosis

Fibrosis is defined as the increase of fibrillar collagen in intermyocardial spaces. Increased fibrosis is recognized as enhancing myocardial stiffness and causing heart failure.[55]

Fibrosis is classified into replacement (secondary) and reactive (primary) types. Scar formation after MI is a typical example of replacement fibrosis. Therefore, fibrosis is often considered to be the end inflammatory reaction. The fibrotic lesions form through multiple steps of synthesis and degradation of various matrix proteins. TN-C is expressed at an acute stage of the cascade, preceding collagen fibril formation.

In the case of reactive fibrosis, collagen fibers increase in perivascular regions without loss of cells and eventually extend among individual cardiomyocytes. It is recognized that inflammation mediated by the renin–angiotensin II–aldosterone system plays a significant role in the progression of this type of cardiac fibrosis. TN-C is expressed at perivascular inflammatory lesions associated with macrophage infiltration (**Figure 3**).

Although it is unclear whether reactive fibrosis is formed through the same molecular mechanism as that of replacement fibrosis, in either case, it is evident that fibrosis and inflammation are closely related, and that TN-C could be involved in the fibrotic process. In fact, deletion of TN-C was shown to attenuate interstitial fibrosis after MI[26] and angiotensin II-induced cardiac fibrosis (Shimojo N et al, unpublished data).

Several studies have demonstrated the interaction of TN-C with ECM molecules, including fibronectin, proteoglycans[10] and periostin;[56] however, the precise role of TN-C in the molecular pathways of collagen fibrillogenesis remains to be determined.

Ventricular Remodeling and TN-C

Ventricular remodeling is clinically manifested as changes in left ventricular chamber volume associated with progressive heart failure after cardiac damage. Biologically, it consists of physiologic and pathologic responses involving structural alternation, characterized by hypertrophy of cardiomyocytes and fibrosis. Recently, the significance of chronic inflammation in

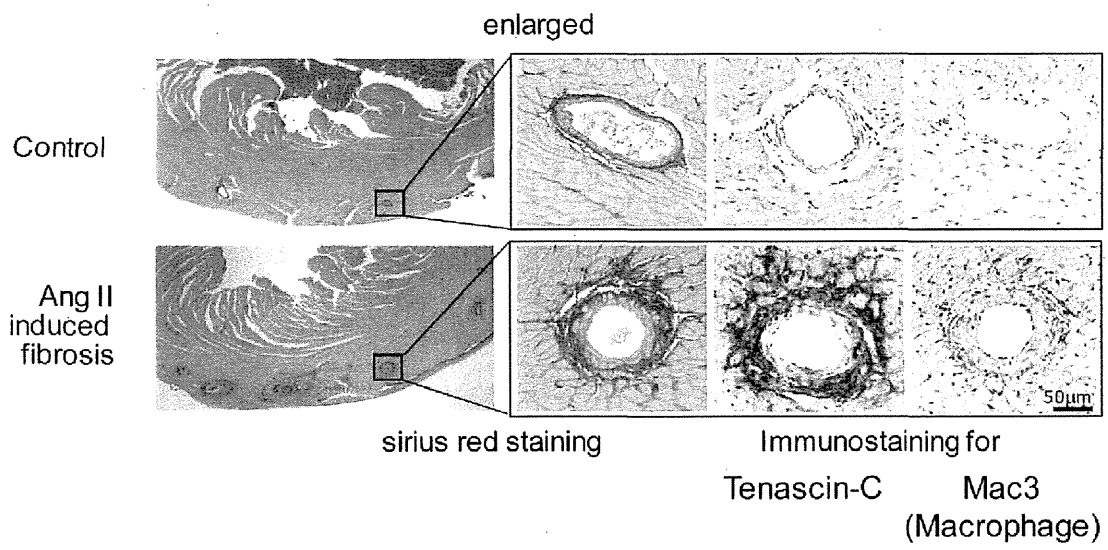

Figure 3. Representative photographs of reactive fibrosis in angiotensin II (AngII)-induced cardiac fibrosis mouse model. (Adapted from Nishioka et al.[41])

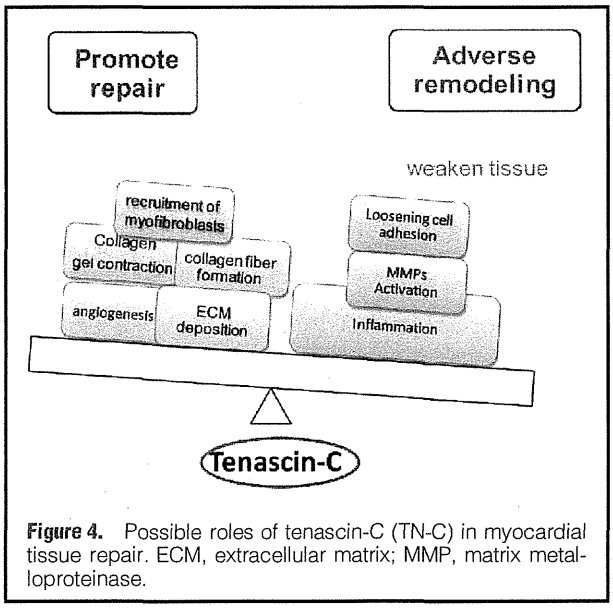

Figure 4. Possible roles of tenascin-C (TN-C) in myocardial tissue repair. ECM, extracellular matrix; MMP, matrix metalloproteinase.

ventricular remodeling has been clarified.[57]

Various remodeling mediators, including proinflammatory cytokines, TGF-β, PDGF, angiotensin II, endothelin-1, hypoxia, and reactive oxygen species (ROS), increase the synthesis of TN-C in vitro.[13,49] In addition to the potential of TN-C enhancing inflammatory responses as discussed earlier, recent studies suggest that TN-C may enhance several signaling pathways, such as endothelin-1/endothelin receptor-A,[58] PDGF/PDGFRβ[31] and transforming growth factor (TGF)-β,[59] in several types of cell. TN-C induced upon inflammation in the heart may modulate ventricular remodeling by controlling these signaling pathways.

This raises the following question: Is TN-C harmful or beneficial for ventricular remodeling? It is difficult to determine this logically, because TN-C has conflicting effects (**Figure 4**). TN-C may loosen cell adhesion, upregulate MMPs, and enhance inflammatory responses. Although these functions help cell rearrangement and allow myofibroblasts and capillary vessels to spread into the tissue under restoration, they might cause tissue vulnerability, resulting in ventricular dilatation. Furthermore, an increase of myofibroblasts and accelerated fibrosis should prevent ventricular dilatation by generating traction forces. On the other hand, excessive fibrosis would lead to stiffer and less compliant ventricles. Moreover, a compensatory system for a lack of TN-C evidently exists. A recent study demonstrated that deletion of TN-C significantly reduced ventricular remodeling and improved cardiac function at day 28 after permanent coronary ligation in mice.[26] Therefore, it appears that TN-C exerts harmful effects for tissue remodeling after infarction, at least in the chronic stages.

Clinical Application

Given its specific expression, TN-C could be a useful marker for evaluating myocardial disease activity. Immunostaining for TN-C significantly improves the sensitivity of a histological diagnosis of myocarditis.[38] The serum level of TN-C measured by enzyme-linked immunosorbent assay may reflect its local expression in the myocardium. For example, serum TN-C in patients with acute MI is significantly elevated, peaks at day 5, and then gradually decreases. Interestingly, patients with high peak levels of TN-C have a greater incidence of ventricular remodeling after 6 months[34] and major adverse cardiac events and poor survival during 5-year follow-up.[60]

Likewise, elevated serum TN-C could be a marker for LV remodeling and a predictor of cardiac events in heart failure in patients with DCM, which is comparable to plasma B-type natriuretic peptide (BNP).[61,62] Particularly interesting is that combining the serum TN-C level with the plasma BNP level is a stronger predictor than either single biomarker alone in

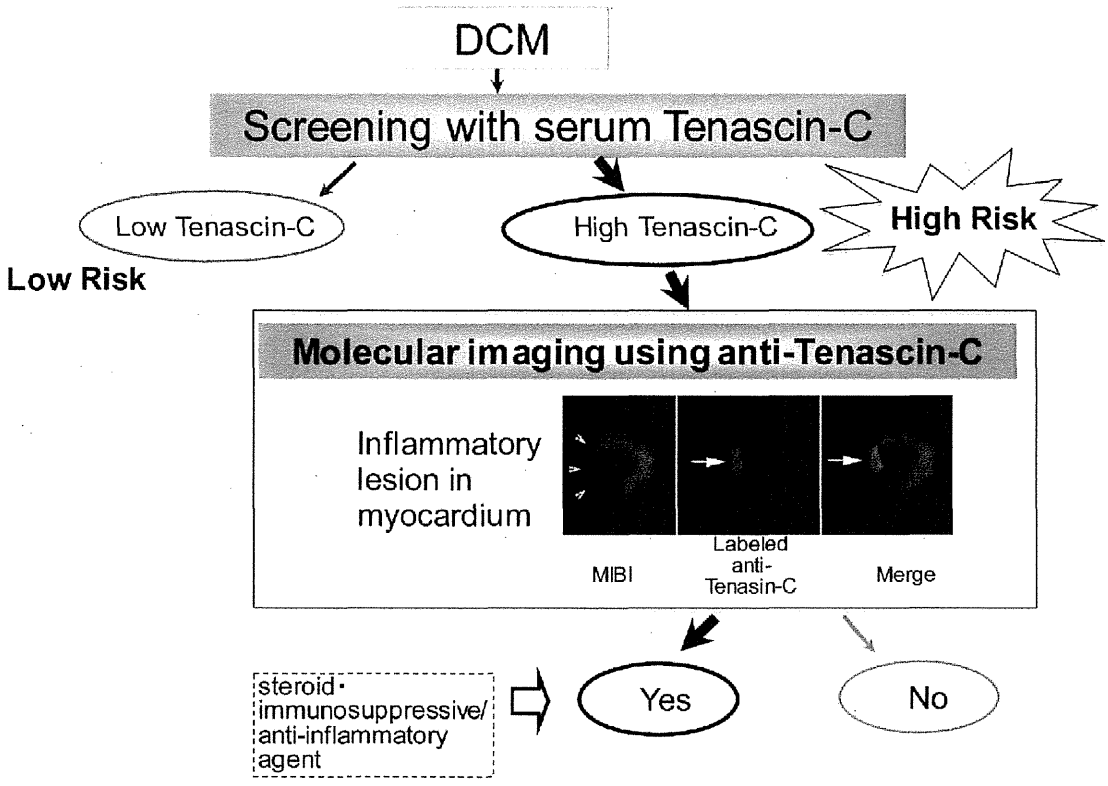

Figure 5. Flow chart for risk stratification and determination of the appropriate therapy for dilated cardiomyopathy (DCM) patients using tenascin-C as a marker.

both acute MI and DCM.[60,62] The combination of BNP secreted from cardiomyocytes and TN-C synthesized in interstitial fibroblasts could enable more precise assessment of the whole heart by reflecting both cardiomyocytes and interstitial cells.

An increasing number of studies have reported the utility as a biomarker of serum TN-C in patients with LV hypertrophy,[63] after resynchronization therapy,[64] supported by mechanical circulatory support devices,[65] with hypertrophic cardiomyopathy,[66] with cardiac involvement of Emery-Dreifuss muscular dystrophy,[67] and with cardiovascular disease of chronic kidney disease.[68] However, TN-C is not synthesized specifically in the myocardium. Normal liver and lung constitutively express TN-C. The elevated levels of circulating soluble inflammatory mediators in heart failure patients might further stimulate secretion of TN-C from the liver or lung. Therefore, it would be necessary to identify the origin of serum TN-C. Molecular imaging could be a promising approach for this. In vivo inflammatory lesions have been successfully imaged in rat models using In^{111}-labeled anti-TN-C Fab'[35,37,40] or single-chain Fv fragments of anti-TN-C.[69]

A precise diagnosis of myocardial inflammation should be important for DCM patients because they may constitute a heterogeneous group, including cases of different phases of inflammatory cardiomyopathy. A recent analysis of myocardium obtained at left ventriculoplasty showed that approximately 50% of 64 DCM patients had significant active inflammation associated with expression of TN-C.[44] A flow chart for risk stratification and determination of the appropriate therapy for DCM patients using TN-C as a marker is proposed (**Figure 5**). Distinguishing inflammatory cardiomyopathy from other types of DCM would improve the management of patients.

TN-C in the Vascular System

Although the expression of TN-C in the vascular system appears a little more complex compared with that in the heart, the expression of TN-C in the normal vascular wall is generally low. High tissue levels of TN-C have been reported within a variety of vascular diseases,[70] including intimal hyperplasia,[21,22,71–79] atherosclerosis,[80,81] pulmonary artery hypertension,[82–84] and abdominal aortic aneurysm.[85–87] A fascinating topic recently reported is that TN-C may be involved in cerebral vasospasm after subarachnoid hemorrhage.[88–91]

Considerable attention has been directed to pulmonary hypertension (PAH). TN-C is upregulated in the vascular lesion[82,84] and may promote proliferation and migration of vascular smooth muscle cells (SMCs),[92,93] a main pathogenic component of PAH. The mutated bone morphogenetic protein type II receptor gene reported in familial PAH induces TN-C transcription,[84] suggesting a direct contribution of TN-C to the progression of PAH.

A recent paper has reported the association of genetic polymorphisms in TN-C and atherosclerosis.[94] The involvement of TN-C in the intimal hyperplasia of occlusive/stenotic vascular disease has also been extensively studied. Intimal hyperplasia is defined as excessive migration and proliferation of SMCs

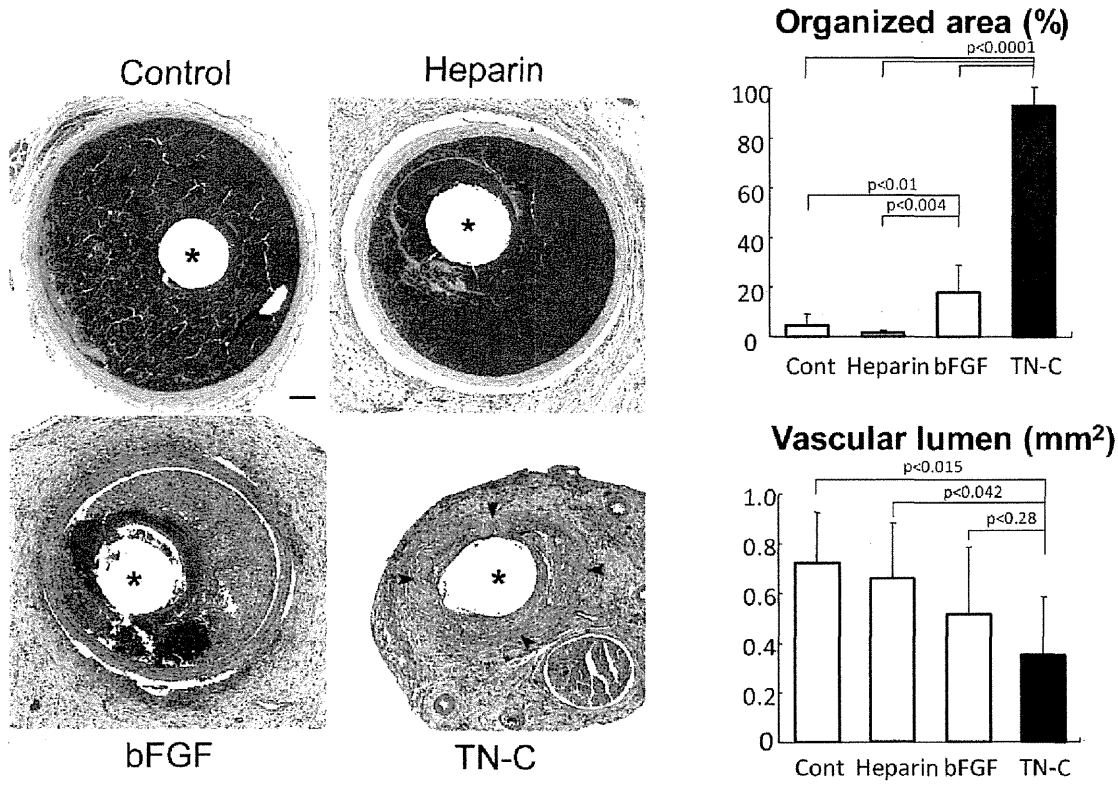

Figure 6. Effect of coil implantation in a rat aneurysm model. The TN-C-coated coil significantly accelerates organization and reduction of the size of the luminal cavity compares with the heparin- or b fibroblast growth factor (bFGF)-coated coil. *Tissue-free area after removal of the coils. TN-C, tenascin-C. (Adapted from Toma et al with permission.[97])

with deposition of ECM proteins. TN-C is expressed in the neointima at an early stage and accelerates progression,[21,22,71-79] and deletion of TN-C reduces intimal lesions.[21,22] Therefore, TN-C may be a target molecule for controlling stenotic neointimal formation. Recent drug-eluting stents have remarkably reduced the rate of restenosis and, at the same time, have created a need for more precise evaluation of pathological change of the lesion combined with vascular imaging.[95] It has been proposed that anti-TN-C molecular imaging of advanced atherosclerotic plaques may be useful[96] for detecting unstable plaque.[80,81] Conversely, the unfavorable function of TN-C to accelerate neointimal formation is applicable to improving the efficacy of endovascular treatment of aneurysms. In fact, treatment of a rat model with TN-C-coated coils remarkably accelerated organization of the cavity and reduction of the lumen size of the aneurysm (**Figure 6**).[97]

Conclusions

TN-C has diverse functions, regulating cell behavior, matrix organization, and inflammation, and should play significant roles during tissue morphogenesis in the embryo as well as in reconstruction of adult tissue after injury. TN-C could exert both harmful and protective effects and might be a therapeutic target as a key molecule in the control of the balance of beneficial and undesirable cellular responses during tissue remodeling.

Furthermore, in view of its specific expression, it is evident that TN-C could be a realistic and promising biomarker and a target for molecular imaging for the diagnosis of various cardiovascular diseases.

Acknowledgments

This work was supported in part by a Grant-in-Aid for Scientific Research from the Ministry of Education, Culture, Sports, Science and Technology of Japan, a research grant for intractable diseases from the Ministry of Health, Labor and Welfare of Japan, and The Okasan-Kato Foundation.

References

1. Bornstein P. Diversity of function is inherent in matricellular proteins: An appraisal of thrombospondin 1. *J Cell Biol* 1995; **130:** 503–506.
2. Bornstein P, Sage EH. Matricellular proteins: Extracellular modulators of cell function. *Curr Opin Cell Biol* 2002; **14:** 608–616.
3. Schellings MW, Pinto YM, Heymans S. Matricellular proteins in the heart: Possible role during stress and remodeling. *Cardiovasc Res* 2004; **64:** 24–31.
4. Matsui Y, Morimoto J, Uede T. Role of matricellular proteins in cardiac tissue remodeling after myocardial infarction. *World J Biol Chem* 2010; **1:** 69–80.
5. Frangogiannis NG. Matricellular proteins in cardiac adaptation and disease. *Physiol Rev* 2012; **92:** 635–688.
6. Okamoto H, Imanaka-Yoshida K. Matricellular proteins: New molecular targets to prevent heart failure. *Cardiovasc Ther* 2012; **30:** e198–e209.
7. Tucker RP, Chiquet-Ehrismann R. The regulation of tenascin expression by tissue microenvironments. *Biochim Biophys Acta* 2009; **1793:** 888–892.
8. Midwood KS, Hussenet T, Langlois B, Orend G. Advances in tenas-